Eötvös Loránd University

Faculty of Science

Centre of Environmental Science

GAMMA SPECTROSCOPY AND EFFICIENCY INVESTIGATIONS USING SEMICONDUCTOR DEVICES

MSc THESIS

OKOLO COLLINS CHUKWUEBUKA

Environmental Sciences MSc

Supervisors:

Csanád Máté, Ph.D.

Associate Professor

and

Veres Gábor, Ph.D.

Full Professor

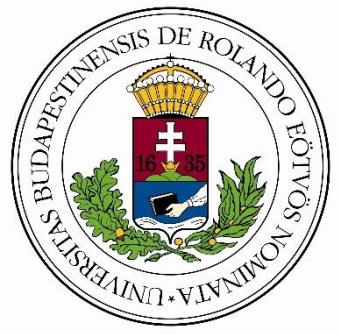

Department of Atomic Physics, Faculty of Sciences, Eötvös Loránd University

Budapest

2021

TABLE OF CONTENTS

Table of Contents

TABLE OF CONTENTS ii

LIST OF FIGURES iv

LIST OF ABBREVIATIONS v

ACKNOWLEDGEMENTS vi

DECLARATION OF ORIGINALITY vii

ABSTRACT viii

1. INTRODUCTION 1

1.1 Overview 1

1.2 Radioactivity in our environment 1

1.3 Motivation for the Thesis 5

1.4 Thesis Outline 7

2. LITERATURE REVIEW 9

2.1 Radioactivity 9

2.2 Types of Radioactive Decay 11

2.3 Interaction of Radiation with Matter 14

2.4 Gamma Spectroscopy 15

2.5 Gamma Spectrometers 17

3. OBJECTIVES 21

3.1 General Objectives 21

3.2 Specific Objectives 21

4. METHODOLOGY AND RESULTS 22

4.1 GEANT4 Application: An Overview 22

4.2 Simulation Results 26

4.3 Laboratory Measurements 33

4.4 Efficiency Calculations and Result Comparison 35

5. DISCUSSIONS 42

6. CONCLUSION 43

REFERENCES 44

APPENDICES 49

Appendix 1: B1ActionInitialization.cc 49

Appendix 2: B1DetectorConstruction.cc – CZT/ CZT in water 50
Appendix 3: B1DetectorConstruction.cc - HPGe 53
Appendix 4: B1EventAction.cc 55
Appendix 5:B1PrimaryGeneratorAction.cc – CZT/ CZT in water 57
Appendix 6: B1PrimaryGeneratorAction.cc – HPGe 59
Appendix 7: B1RunAction.cc 60
Appendix 8: B1SteppingAction 63
Appendix 9: HPGeAutoRun.mac 65
Appendix 10: KromekAutoRun.mac 66
Appendix 11: run1.mac 67
Appendix 12: draw662keV.C 68
Appendix 13: DrawAllE.C 69
Appendix 14: DrawEffPlot.C 71
Appendix 15: DrawGausFit 72

LIST OF FIGURES

Figure 1: Global estimates of annual radiation exposure from various sources expressed in both mSv and percentages of the total exposure. For Germany, “Other” incudes fallout resulting from nuclear tests, to the Chernobyl accidents, and to the releases from nuclear power plants. (UNSCEAR 2008)3
Figure 2: Relative priority of processes by which gamma-rays interact with matter. 17
Figure 3: Schematic diagram of NaI(Tl) scintillating detector (Courtesy of AMPTEK, GammaRad5 Manual) 18
Figure 4: Kromek GR1 Spectrometer built with a 1cm^3 CZT detector (Amman, 2017). 19
Figure 5: Amptek's PX-5 HPGe detector schematic diagram (Courtesy of Amptek) 20
Figure 6: Mandatory User Classes 22
Figure 7: GEANT4 Application Architecture (Simone 2008) 23
Figure 8: Application flowchart showing mandatory components and the actions they perform. 24
Figure 9: Visualization of the (10x10x10) mm CZT detector 24
Figure 10: Visualization of the HPGe detector with outer radius 2.5 cm and inner radius 0.2 cm ... 25
Figure 11: B1RunManager flowchart 25
Figure 12:Visualization of incoming photons on the CZT detector during simulation 27
Figure 13: Distribution of incoming photons on the face of the detector. 27
Figure 14: Combined histogram of energy deposition by incoming photons for 38 different energies in air 28
Figure 15: Distribution of incoming ~662 keV photons on the face of the detector. 28
Figure 16: Energy deposition histogram for the ~662 keV photons in air 29
Figure 17: Energy deposition histogram when CZT immersed in water. 29
Figure 18: Visualization of the HPGe detector showing incoming photons. 30
Figure 19: X-Y coordinates of incoming photons 31
Figure 20: HPGe energy deposition histogram in air 31
Figure 21: X-Y distribution of incoming photons of ~662 keV 32
Figure 22: Histogram showing energy deposited against incoming energy of 662 keV in air. 32
Figure 23: Laboratory setup using Cs-137 as radioactive source 60 cm away from Kromek GR1 detector 34
Figure 24: Output from Kromek KSpect Analyzer for Cs-137 source 35
Figure 25: Efficiency plots of simulation cases with combined energies 38
Figure 26: Cs-137 as a point source radiating equally in all directions around a sphere. 39
Figure 27: Kromek spectrum full energy peak with Gaussian fit 40

LIST OF ABBREVIATIONS

ALARA	As low as reasonably achievable
CdZnTe	Cadmium Zinc Telluride
CERN	European Council for Nuclear Research
CZT	Cadmium Zinc Telluride
FWHM	Full width at half maximum
GPS	General Particle Source
LN_2	Liquid nitrogen
MCA	Multichannel analyzer

ACKNOWLEDGEMENTS

I would like to express my deepest and profound gratitude to my supervisor, Professor Csanád Máté and co-supervisor Veres Gábor for the very well-structured guidance provided to me during the research. Their spirit of enthusiasm, courage, and discipline in research rubbed off on my personality and, the technical and analytical skills I have gained during this research has made me more confident.

I would like to thank the Director of the Center of Environmental Sciences at ELTE, Professor Tamás G. Weiszburg whose unique and interesting teaching, examination, and problem-solving methods has fostered a spirit of scientific thinking in me. The profound tutelage, advice, and field trips he provided to us during the MSc program made learning quite interesting and adventurous and this has left a positive impact.

I would also like to express my sincere appreciation to Lökös Sándor for the assistance he provided during the laboratory measurements; Professor Horváth Ákos for setting up a GEANT4 working group at the early stages of my thesis work, where we discussed and solved GEANT4 related problems by assisting and learning from others; and Erzsébet Harman-Tóth for her support and proper dissemination of useful information.

My heartfelt appreciation goes to the Hungarian Government and Eötvös Loránd University for providing the opportunity to obtain this diploma under a full scholarship.

I would also like to thank my supportive managers and exceptional teammates at Morgan Stanley for their support and flexibility to my work schedule during my research.

I am indebted to my family; my father, Collins Okolo, my mother Adeline Okolo and all my siblings who always supported me through thick and thin.

Finally, I would like to thank my lecturers for selflessly imparting very practical and useful knowledge and to my friends for the support and motivation.

DECLARATION OF ORIGINALITY

Name: Okolo Collins Chukwuebuka

Neptun ID: NU924V

ELTE Faculty of Science: Environmental Science, MSc

Specialization: Environmental Physics

Title of diploma work: Gamma Spectroscopy and Efficiency Investigations using Semiconductor Devices.

As the author of the diploma work, I declare with disciplinary responsibility that my thesis is my own intellectual product and the result of my own work. Furthermore, I declare that I have consistently applied the standard rules of references and citations.

I acknowledge that the following cases are considered plagiarism:
– using a literal quotation without quotation mark and adding citation;
– referencing content without citing the source;
– representing another person's published thoughts as my own thoughts.

Furthermore, I declare that the printed and electronical versions of the submitted diploma work are textually and contextually identical.

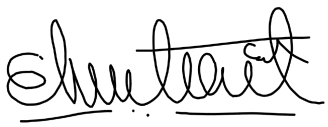

Budapest, 2021

Signature of Student

ABSTRACT

Radiation emissions from both natural and anthropogenic sources is inevitable in the world today. Advancements in nuclear research has given rise to applications of radioactivity in many areas. As these applications of radioactivity continues to grow, the importance of advanced, accurate, and reliable in-situ measurement techniques cannot be overemphasized. Innovative technologies have made it possible to fabricate portable gamma ray detectors at a commercial level and this thesis explores the practicability of such detectors. Two types of gamma spectrometers were used for this purpose: a Kromek CZT detector and the Canberra HPGe detector. The efficiencies of these detectors were obtained using GEANT4 simulations first, and then compared with the efficiencies obtained from actual physical measurements. The comparable results obtained from the simulations and measurements demonstrate that these detectors are practicable for photon detection and measurement, although there is a need for further advancements to improve efficiency.

1. INTRODUCTION

1.1 Overview

Radiation emissions from both natural and anthropogenic sources is inevitable in the world today. Radioactivity has existed from the formation of the earth and radioelements are present in the rocks and soil we walk and live upon, the food we eat, the water we drink, and even in the air we breathe. Radiation also exists in outer space and in fact, the sun which is the most important source of energy supporting life on earth constantly emits a type of radiation known as the cosmic radiation.

Advancements in nuclear research has given rise to applications of radioactivity in many areas such as medicine, archeology, power generation, warfare, food production, and manufacturing to mention but a few. These applications have benefits which has advanced the way humans live and operate but it also has its risks and as we have seen in the past with the Chernobyl and Fukushima disasters, the results can be very catastrophic. Therefore, it is very important to understand and regularly investigate both the sources and applications of radioactivity in our environment while complying strictly to maintain radiation levels to as low as reasonably achievable (ALARA) in order to leverage the benefits while mitigating the associated risks as much as possible.

In order to apply the ALARA principle effectively, efficient and reliable measurement techniques and devices must be used to accurately investigate sources of radiation from both natural and artificial sources to ensure that the most reasonable minimum limits which support the sustenance of a healthy life are maintained.

1.2 Radioactivity in our environment

We encounter radiation in our everyday life from various sources. It is even almost impossible to talk about the formation of the earth and its environment in scientific terms without mentioning radioactivity. Kirshner R.P. (2014) suggests that radioactivity predates the existence of earth and life on earth. The study even goes on to claim that the elements that make up the earth and its inhabitants was created in a violent radioactive environment. Most elements from these events have become stable but there are several other unstable

isotopes of some elements that are still in existence today, most notably uranium-235, uranium-238, thorium-232, and potassium-40 which all have a long half-life.

Radionuclides can be found in rocks and soil, in food, water, air, and even in our bodies! Majority of human radiation exposure emanate from natural sources, but it can also be artificial as in the case of radiation applied in areas such as in medicine and in nuclear power plants. The origins of radiation that constitute the background radiation is prevalent everywhere on earth, although the distribution of these sources vary according to location (Kovler et al, 2017).

According to (IAEA, 2011), "there are four main components of general background radiation:

i. Natural radioactivity in food and water and inhaled air.
ii. Natural terrestrial radiation from our immediate environment, including buildings.
iii. Natural cosmic radiation from Sun, stars and from galactic and intergalactic plasma.
iv. Medical and industrial applications."

The Figure 1 below shows the estimates of the global radiation exposure originating from both natural and artificial sources according to the UNSCEAR 2008 report.

As can be observed from Figure 1, radon constitutes the largest source of human exposure to radiation. Radon-222 is an inert, colorless, odorless and tasteless gas resulting from the decay from uranium-238. Radon can escape the rocks and soils from which it is produced and can diffuse out into the air of soils by convection and then into both the indoor and open air (Csanád et al., 2012). In fact, soil gas containing radon is the predominant source of indoor radon and research has proven that it can cause serious health issues (and even death) when it is inhaled into the human body, making it the second most important cause of lung cancer after smoking (Samet, 2011). Radon levels that escape indoors increases during the winter months when indoor buildings are usually sealed (Vogeltanz-Holm et al., 2018). Several studies (Fonollosa et al., 2016; Moreno et al., 2014; Jobbágy, 2017) has shown that radon is introduced into water by natural processes involving decay of radium-226 which is also part

of the uranium-238 decay series and prevalently from rocks and soils in the surrounding environment. Airborne radon may also dissolve into water and other water in-flows in the catchment area with higher radon (Jobbágy, 2017). The chemical and physical properties of radon as well as its prevalence makes it an important aspect of environmental investigations by environmental scientists who measure and monitor the radiation levels in the environment in which we live.

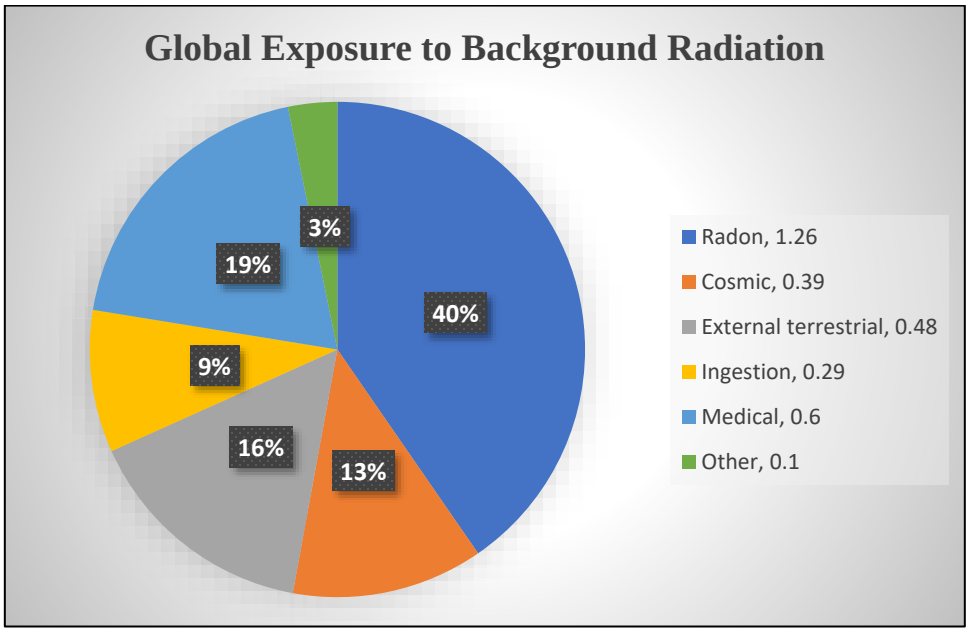

Figure 1: Global estimates of annual radiation exposure from various sources expressed in both mSv and percentages of the total exposure. For Germany, "Other" incudes fallout resulting from nuclear tests, to the Chernobyl accidents, and to the releases from nuclear power plants. (UNSCEAR 2008)

Cosmic radiation is an ionizing radiation that has its origins from the Sun and from extra-terrestrial sources both within and outside our solar system. Cosmic radiation is produced when primary photons and α particles from outside space interact with components of the earth's atmosphere (Bagshaw, M. 2019). These protons can possess very high kinetic energy much larger than it is possible to produce in particle accelerators by man, although this is rare (Csanád et al., 2012). It is important to note that cosmic rays do not originate from radioactive decay like most other sources previously mentioned above, however when these fast-moving rays interact with the atmosphere nuclear reactions can occur. Exposure to cosmic radiation is an important aspect of air transportation which must be carefully measured and monitored. (Spurný 2001) classified the sources of radiation exposure during

space flights and at high altitudes into three: galactic cosmic radiation, solar cosmic radiation and radiation of the earth's radiation belt (Van Allen belts).

Food consumption is another source of exposure to the natural background radiation. Crops obtain their nutrients from the soils which contain radionuclides as has been previously described in previous sections of this chapter. These radionuclides from soils and rocks are then transferred to the surrounding freshwater, lakes, and rivers as well as to crops and fishes during growth. Banana and Brazil nuts are well known sources of foods that contain substantial amounts of radioactivity (EPA, 2019).

Radiation is applied in the field of medicine for diagnosis and treatment of various diseases and defects. From Figure 1, it is observed that radiation in medicine is the most important source of radiation exposure from an anthropogenic source. X-rays possess ionizing high-energy and due to their high penetrating nature, they can be used for inspection of internal bones and tissues. Radiation therapy is important in the treatment of cancer with nearly 50% of all cancer patients receiving this form of therapy during their illness. It is worthy to mention that this provides abouts 40% of curative treatment for cancer (Baskar et al., 2012). During treatment, radioactive beams of intense energy are used to either kill or control malignant cells and inhibit their multiplication (cell divisive) potential. Radiation therapy has also been employed in non-malignant diseases. In Germany, non-malignant indications for radiotherapy constitutes about 10–30% of all treated patients in most academic, public and private radiotherapy facilities (Seegenschmiedt et al., 2015).

Technological advancements have made it possible to apply radioactivity in various industries such as in the power and agro industries, in manufacturing, military, transportation, and even in environmental protection. In order to curb the huge environmental pollution resulting food packaging, Canada is carrying out research with the aim to develop biodegradable, eco-friendly food packaging using radiation technology (IAEA 2017).

Radiation is used in science and medicine to obtain projection data through computerized tomography; the process of acquiring the distribution of density within a human body with the aid of multiple X-ray projection (Herman Gabor, 2009).

Less than two years after the first demonstration of self-sustaining nuclear reaction by Enrico Fermi in Chicago on December 2, 1942, nuclear energy was used to create the first atomic bomb under the code name *Manhattan Project* which was deployed on July 16, 1945 in Hiroshima, Japan during the Second World War (U.S. DOE, 2011). A year later the Atomic Energy Commission (AEC) was created by the U.S. Congress to promote the development and use of nuclear energy for peaceful purposes. Subsequently, in 1957 the first commercial nuclear power plant was completed in Shippingport, Pennsylvania. Today, about 440 nuclear power reactors generate an estimated 10% of the world's electricity with about 50 more reactors under construction having a capacity which is equivalent to approximately 15% of existing capacity (World Nuclear Association, 2021).

Generation of electricity from nuclear energy has resulted in nuclear disasters in the past; most notably, the Chernobyl disaster and the Fukushima Daiichi nuclear disaster on April 26, 1986 and March 11, 2011, respectively. The most severe nuclear accident in the history of civilian nuclear power ever recorded is the 1986 Chernobyl accident which released a collective dose many times higher than the combined collective dose from all other accidents causing radiation exposures to the general population (UNSCEAR 2008). According to (Beresford et al., 2016), "The Chernobyl accident led to a large resurgence in radioecological studies both to aid remediation and to be able to make future predictions on the post-accident situation, but, also in recognition that more knowledge was required to cope with future accidents."

1.3 Motivation for the Thesis

The events narrated above clearly shows why it is important to constantly adhere strictly to medical, environmental and governmental regulations when dealing with significant amounts of radiation. The tricky nature of a radioactive source gives it the ability to emit ionizing radiation which cannot be detected or "felt" by the human senses but capable of causing serious health issues. Therefore efficient, reliable, and continuous monitoring is required by governments and agencies and the importance of real-time in-situ detection and measurement devices and techniques cannot be overemphasized. This can prevent the transportation of potentially harmful materials to laboratories while also minimizing both time of exposure and the number of people exposed. Safety provided to environmental

researchers and indeed the entire population can be enhanced by deploying efficient means of detecting and investigating the composition of radioactive sources.

This thesis will carry out an investigation on the efficiencies of two types of semi-conductor gamma-ray spectrometers: the Kromek (GR1) and the HPGe detectors. To the best knowledge of the student at the time of writing this report, the Kromek CZT (or CdZnTe – Cadmium Zinc Telluride)-based GR1 and GR1-A are "the world's smallest and highest resolution room temperature gamma-ray spectrometers" commercially available (Kromek, 2016). The Kromek is a completely self-contained $1cm^3$ CZT (or CdZnTe – Cadmium Zinc Telluride) solid state detector equipped with a built-in preamplifier, shaping amplifier, baseline restorer, pulse height digitizer, and HV supply (Kromek, 2016). The detector is powered by a computer to which it is connected via USB during measurement through which the digitized pulse heights of detected gamma-ray signals are transferred. The student believes such portable gamma-ray spectrometers will advance the way environmental researchers carry out in-situ investigation in real-time.

The HPGe detector is a high-purity germanium detector known to have high efficiencies as will be displayed in the simulations and laboratory measurements. The HPGe detector has a higher sensitive thickness when compared to the Kromek detector and as a result it can detect and measure higher energy photons which gives it a better resolution. The main disadvantage of this detector is that it requires cooling by liquid nitrogen (LN_2). This will be demonstrated in subsequent chapters of this thesis work.

Knowing the type and number of radioactive components in materials in important because of two reasons:

- identifying composition, as this can help to determine the origin of an object, where it was made, or even when it was made (because radioactive decay helps us telling the age of objects)
- knowing how radioactive they are, i.e. how much radiation comes out of them and at what energies.

Knowing these amounts is only possible if we know efficiency and its energy dependence. Determining efficiency for many energies is not easy experimentally, we would need to have many sources (emitting photons at different energies) with very well-known activity. Hence determining efficiency with simulations is an important and useful tool. Simulating detectors is also important from other points of view, like understanding how much secondary radiation they create, etc; but for this thesis, we focus on efficiency determination.

The efficiencies of both detectors will be determined based on simulations using GEANT4, a toolkit developed by the European Council for Nuclear Research (CERN). Afterwards, we will compare the simulated results with those obtained from actual physical laboratory measurements.

1.4 Thesis Outline

This thesis which is divided into six chapters promises to be interesting. The first chapter gives a general introduction to radioactivity. Several applications of radioactivity as well as the sources contributing to the background radiation was discussed at a high level. This chapter also describes the motivation of the student in carrying out his thesis in this subject which is to analyze the applicability and efficiency of advanced portable gamma-ray spectrometers for in-situ detection and investigation of radioactive sources in the environment.

The second chapter continues the review of literature which was performed to an extent in chapter 1 but with a more scientific approach; applying physical and chemical equations from both physics and nuclear chemistry. The student leveraged previous works by various researchers in formulation of this thesis which also demonstrates the knowledge gained by the student during his studies and research. The sources cited include those from journal publications, textbooks, and official websites of established scientific institutions and government agencies. The third chapter clearly states the general and specific objectives of this thesis work.

The fourth chapter describes the methodology used to obtain the results obtained from GEANT4 simulations and laboratory measurements at the Institute of Physics located in the Faculty of Sciences of Eötvös Loránd University. The results are also given in this chapter.

In chapter five, the student makes meaning and importance out of the obtained results in relation to the literature review in chapter two and to support the conclusion in chapter six.

2. LITERATURE REVIEW

A description of radioactivity has been given in a broader sense in chapter one; including some of its sources in the environment, the benefits and applications in several fields as well as some of its consequences. The reader may be curious and even skeptical and poised to raise the questions: "How is all this even possible? How exactly does these phenomena occur?" Therefore, in this chapter, we will explore radioactivity with a more scientific approach.

2.1 Radioactivity

Unstable nuclei such as the nuclei of uranium-235 undergo decay during which particles and ionizing electromagnetic radiation are emitted. Therefore, radioactivity can be defined as the spontaneous emission of particles and electromagnetic radiation from nuclei of unstable atoms (Ball et al., 2014).

The activity, *A* is the number of disintegration or decay occurring per second in the nucleus of an unstable atom. The SI unit of activity is Becquerel (Bq). Mathematically,

$$A = -\frac{dN}{dt} \tag{1}$$

N is the number of radioactive nuclei about to disintegrate, *t* is time in seconds.

Equation (1) implies that although the activity is positive, the number of disintegrations occurring in the nuclei decreases with time. In a decay chain for a daughter isotope the change in the number of these nuclei can be due to the decay but also due to their production from the mother nucleus, as well. Therefore, above formula is valid only for simple decays because the change in the number of nuclei undergoing decay in a daughter isotope can be as a result of the decay itself as well as due to its production from the mother nucleus (Csanád et al., 2012).

The relationship between the activity and the number of disintegrations in the nuclei can be expressed as:

$$A = \lambda N \qquad (Bq) \tag{2}$$

where, λ is the decay constant which is the probability of decay (or disintegration) per unit time; its unit is *per second* (s^{-1}).

The relationship in (2) demonstrates that the nuclear decay is a purely statistical phenomenon.

Equations (1) and (2) can be related in differential terms,

$$\frac{dN}{dt} = -\lambda N \tag{3}$$

Solving the differential equation in (3) for a simple decay process we obtain,

$$N(t) = N_0 e^{-\lambda t} \tag{4}$$

This is known as the *exponential decay law* and it demonstrates the number of radioactive atoms decaying exponentially with respect to time. $N(t)$ is the number of atoms available after a time *t* and N_0 is the initial number of decaying atoms at initial time.

From (4), we can determine the number of atoms present in a radioactive sample after a specified time and we can also determine the number of atoms that have decayed within a given time prior to the collection of the sample.

By taking the derivative on each side of (4) with respect to time we obtain:

$$N'(t) = -(-\lambda) N_0 e^{-\lambda t} \tag{5}$$

Recall from (3) that: $N(t) = N_0 e^{-\lambda t}$. Substituting this into (5) we obtain:

$$A(t) = \lambda N(t) \tag{6}$$

If the number of atoms available after a time *t* is half its original value, we can express (4) as:

$$\frac{N_0}{2} = N_0 e^{-\lambda T_{\frac{1}{2}}} \tag{7}$$

where $T_{\frac{1}{2}}$ is the amount of time it takes half of the original number of nuclei to decay; this is known as the *half-life* and it is a term which is usually used to describe how quickly decay occurs in radioactive samples. Some radioisotopes have a short-half life such as polonium-210 (138 days), while others have a very long half-life such as uranium-235 (about 703 million years).

Solving (5) by taking the logarithm of both sides we obtain:

$$\lambda = \frac{ln\ 2}{T_{\frac{1}{2}}} \tag{8}$$

This formular illustrates the inverse relationship between the decay constant of a radioactive material and its half-life implying that a radioactive source with high decay rate (or decay constant) will have a shorter half-life than a source with a lower decay rate.

In a radiation detector, the counting rate, *C*, is equal to the activity of the radioactive nuclei present in the radiation source multiplied by a constant which relates to the efficiency of the detector (Loveland et al., 2005). Thus,

$$C = \varepsilon A = -\varepsilon \frac{dN}{dt} = \varepsilon \lambda N \tag{9}$$

Where ε is the efficiency. Substituting (9) into (4) we obtain,

$$C(t) = C_0 e^{-\lambda t} \tag{10}$$

2.2 Types of Radioactive Decay

(Thomson, 1897) carried out a cathode ray experiment to study the cathode ray and discovered that they are made up of negatively charged particles, which are called *electrons* today. (Rutherford, 1911) proposed the atom model with the gold-foil experiment giving the theory on the structure of atoms. This theory states that the atom comprises positively charged nucleus which is surrounded by a system of electrons held by attractive forces from the nucleus. This positively charged particles are now referred to as *protons*. (Bohr, 1913) built on the research carried out by Rutherford and proposed the Bohr (or Bohr-Rutherford) model. This model comprises a system of orbiting electron surrounding a dense nucleus. Further research carried out by one of Rutherford students, James Chadwick proved the existence of electrically neutral particles called *neutrons* in the atomic nucleus (Chadwick, 1935). These works carried out by these outstanding scientists form the basis of nuclear physics today.

The sum of protons and neutrons present in a nucleus of an atom is known as the mass number, (*A*) and the atomic number (*Z*) denotes the number of protons present in the nucleus.

When nuclei of radioactive sources undergo disintegration (or decay) a change in the atomic structure is expected but this is not so in the case of gamma radiations. The particles

emitted during such decay determines what kind of change will occur in the nucleus. There are three types of radioactive decay: the alpha decay, the beta decay, and the gamma decay.

2.2.1 Alpha decay (α-decay)

During an alpha decay, the nucleus disintegrates to emit an alpha particle, i.e., the helium nucleus, ${}^{4}_{2}He$ which has two protons and two neutrons. The nucleus thereby decreases its atomic number by 2 and its mass number by 4. The general equation is written as:

$$ {}^{A}_{Z}X \rightarrow {}^{A-4}_{Z-2}X' + \alpha \tag{11} $$

where *X* is the mother nucleus and *X'* is the daughter nucleus. Thorium-234 is produced by an alpha decay from its mother nucleus, uranium-238 as shown in (10) below.

$$ {}^{238}_{92}U \rightarrow {}^{234}_{90}Th + {}^{4}_{2}He \tag{12} $$

Thorium-234 is called the daughter nucleus of uranium-238 because it is produced from it in this reaction. Radon-222 is also produced in a similar fashion from the radium-226 isotope.

Alpha particles are usually not harmful to touch because they can lose most of their energy within a very small volume of a material and can even be shielded by piece of paper. However, when ingested into the body they can result in serious health issues such as cancer as in the case of Radon. When ingested, radon which has a half-life of 3.8 days and its daughters will deposit energy to body cells resulting in radon-associated cancer (National Research Council, 1999). Elaborate laboratory research conducted using single alpha particles shows that one-hit of an alpha particle to a cell can result in a permanent change to that cell and can cause "by-stander" effects on adjacent cells (Samet, 2009).

2.2.2 Beta decay (β-decay)

In a beta decay, the atomic number increases or decreases by 1 while the mass number remains unchanged. It can be said that two particles are "created" during this process when compared with the "disruption" of a heavy nucleus that occurs in α-decay making the beta decay more complicated than the alpha decay (Loveland et al., 2005). At a high level, we will focus on the beta-minus (β^-), the beta-plus (β^+) decay and the electron capture (EC).

In the β^- decay, the atomic nucleus is changed with its atomic number increasing by 1 with the emission of an electron (e^-) and an antineutrino ($\bar{\nu_e}$). The general formula for a beta-minus decay is:

$$ {}^{A}_{Z}X \rightarrow {}^{A}_{Z+1}X' + e^- + \bar{\nu_e} \tag{13} $$

The beta-minus decay can be used to describe the process in which a neutron is converted into a proton with the "creation" of an electron and its antiparticle – the antineutrino. A neutron undergoes β^- into a proton through this process, thus:

$$ {}^{1}_{0}n \rightarrow {}^{1}_{1}p + {}^{0}_{-1}e^- + {}^{0}_{0}\bar{\nu}_e \tag{14} $$

In the β^+ decay, a proton is converted to a neutron and the atomic nucleus is changed with its atomic number decreasing by 1. During this process, a positron (e^+) and an electron neutrino (ν_e) is emitted. The general formula for a beta-plus decay is:

$$ {}^{A}_{Z}X \rightarrow {}^{A}_{Z-1}X' + e^+ + \nu_e \tag{15} $$

A proton undergoes β^+ decay to be converted into a neutron, thus:

$$ {}^{1}_{1}p \rightarrow {}^{1}_{0}n + {}^{0}_{+1}e^+ + \nu_e \tag{16} $$

There is a third process which is especially important for heavy nuclei; it is called the electron capture (EC) and it is the process by which an orbital electron is captured by a proton in the nucleus (Loveland et al., 2005). The equation is written thus:

$$ {}^{A}_{Z}X \rightarrow {}^{A}_{N+1}X' + \nu_e \tag{17} $$

This final state of this process also has only two products and therefore conservation of momentum will cause the neutrino to be emitted with specific energies depending on two factors; the binding energy of the electron captured and the final state of the daughter nucleus (Loveland et al., 2005).

2.2.3 Gamma decay (λ-decay)

In a gamma decay, both the atomic number and mass number remains unchanged, however energy is released during the process. λ-decay occurs when excess energy is released by an excited nucleus thereby emitting electromagnetic radiation, that is, a photon (Loveland et al., 2005). The equation is written thus:

$$ {}^{A}_{Z}X \rightarrow {}^{A}_{N}X' + \gamma \tag{18} $$

X' indicates a de-excitation from its original excited state to a lower energy state. Gamma decay can be observed after other decay such as the alpha and beta decays because the daughter nucleus is often in an excited state. These nuclei emit photon in order to attain a lower energy state and the emitted photon interact with the medium in which they travel.

2.3 Interaction of Radiation with Matter

Electromagnetic radiation interacts with the medium in which they travel through a process known as *ionization*. Ionization can be defined as a process by which photons transfer their energy to an electrically neutral atom when it acquires a positive or negative charge resulting in the formation of *ions*. Bremsstrahlung, or continuous X rays result from the acceleration of free electrons or other charged particles (Evans, 1955).

The range indicates the distance the formed ions can travel until they attain room temperature or the temperature of the medium (Csanád et al., 2012). The range is 10 μm for natural alpha-radiations within the energy range of 5-10 MeV range; in air, with 1000 times lower density, it is 3 – 10 cm; and the range is about several centimeters for electrons from beta-decays (Csanád et al., 2012). It is important to note that the range is affected by the nature of the medium and in a material that contains quite several electrons (Csanád et al., 2012). There are three mechanisms that can occur when a photon interacts with matter, they are: the photelectric effect, Compton scattering and pair production. These mechanisms are dominant at energies exceeding the ultraviolet range.

The cross-section of a material determines the probability of atomic processes that occur in it. The number of reactions, N_r in a unit time is given by:

$$N_r = \sigma I \rho dx \tag{19}$$

where σ is the cross-section of the medium, ρ is the density of the medium, dx is the thickness of the cross-section, and I is the radiation intensity which is given by:

$$I = \frac{\Delta \mathrm{N}}{\Delta t} \tag{20}$$

where N is the number of photons passing through at time interval Δt.

If equations (19) and (20) is solved further, we will be able to express I as:

$$I(x) = I_0 e^{-\sigma\rho x} \tag{21}$$

The multiplication of the medium's cross-section and density gives the attenuation coefficient, μ. Thus,

$$\mu = \sigma\rho \tag{22}$$

Substituting (22) into (21),

$$I(x) = I_0 e^{-\mu x} \tag{23}$$

This is important because radioactive sources produce photons of characteristic energy and intensities and through proper detection and analysis, a gamma spectrum can be created which is characteristic of that radioactive source. One of the methods used to detect and investigate composition of samples is *gamma spectroscopy*.

2.4 Gamma Spectroscopy

The radioactivity in a sample is determined using gamma spectroscopy. Gamma spectroscopy is a quantitative non-destructive analytical technique used in the detection of photons from radioactive sources and it is usually used to investigate the composition of radioisotopes present in a sample by inspecting its full energy peaks.

Gamma spectrometry has so many useful applications in geology, nuclear industry and astrophysics. This technique is particularly useful in scenarios where nondestructive measurements and analysis is quickly required using gamma spectrometers or gamma-ray detectors.

In section 2.3 the process of radiation interaction with matter was explained and the possible mechanisms that can occur when photons pass through a medium were stated. Now, we will take a closer look at these mechanisms.

2.4.1 Photoelectric effect

The photoelectric effect is the phenomenon that occurs when the absorbed photon transfers its total energy to a bound electron that is then ejected from its location. Both the photon and ejected electron acts as a wave because the energized electron will ionize several electrons along its path within a short distance until total energy transfer is achieved.

The cross section or probability of the photoelectric effect has a glaring dependence on the atomic number of the absorbing material with sharp increase observed in the cross-section at each threshold for the emission of bound electrons (Loveland et al., 2005).

2.4.2 Compton scattering

The Compton effect occurs when a photon strikes a weakly bound electron thereby transferring some of its energy and then deflected to a different direction (Csanád et al., 2012). The cross-section for Compton scattering is proportional to the atomic number *Z* of the absorbing medium.

2.4.3 Pair production

Pair production or formation of electron-positron is possible in the electric field of the atomic nucleus for photons that possess energy great than the 1.022 MeV threshold; the photon is annihilated during this process and due to the conservation of energy and momentum, the created electron and positron will move forward along the direction of the destroyed photon with an opening angle between them (Loveland et al., 2005). The probability this mechanism has an absolute dependent on the 1.022 MeV threshold and therefore cannot take place for photons possessing lower energies (Loveland et al., 2005).

These three phenomena – photoelectric effect, Compton scattering, and pair formation – are of high importance when choosing the absorbing materials of detectors. As previously explained, the precedence for each of this process is dependent on the photon energy and atomic number. Figure 2 below illustrates the relative priority as a function of atomic number and photon energy (Loveland et al., 2005)

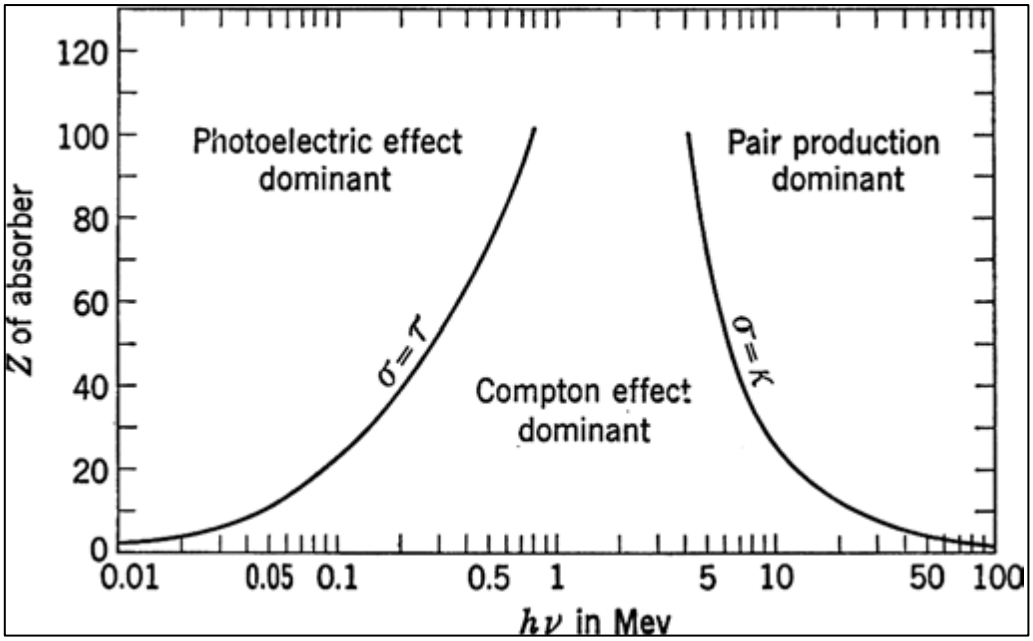

Figure 2: Relative priority of processes by which gamma-rays interact with matter.

2.5 Gamma Spectrometers

The fundamental components of gamma-ray spectrometer systems include a spectrometer, an amplifier, data processing equipment, bias supply, system power supply, and auxiliary equipment such as cables, tripods, shielding, etc. (Shebell, 1999). Two types of gamma spectrometers are discussed below.

2.5.1 Scintillation Detector

Scintillation is the process by which some material known as a scintillator emits light in response to incident ionizing radiation with an emission corresponding to a detection event. The NaI(Tl) scintillator is usually used in practice and is made of sodium iodide (NaI) doped with thallium (Tl). This NaI(Tl) crystal is coupled to a photomultiplier tube which converts the small flashes of light into electrical signals by photoelectric effect (Pavan et al., 2019). Figure 3 shows the schematic diagram of this detector.

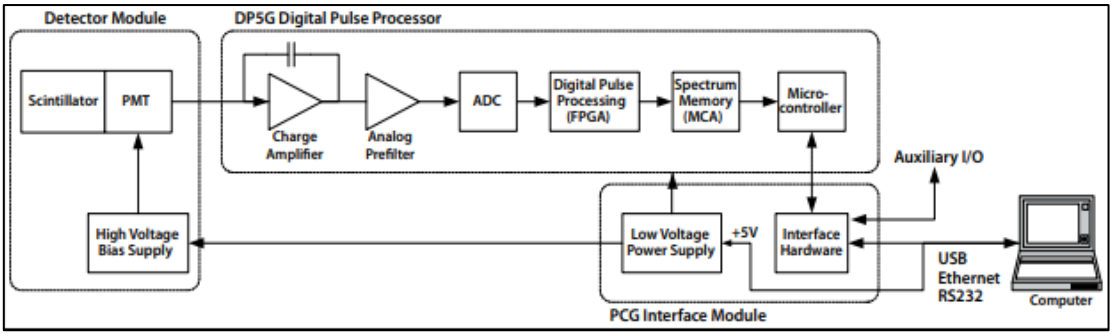

Figure 3: Schematic diagram of NaI(Tl) scintillating detector (Courtesy of AMPTEK, GammaRad5 Manual)

2.5.2 Semiconductor Detector

The change in conductivity of certain semiconductors when hit by an incoming photon can be converted into electrical pulses that is used to detect and investigate radiation. There is a small energy gap between the valence band of electrons and the conduction band and when impacted by an incoming photon, the energy passed is enough to promote electrons to the conduction band which results to a change in conductivity (Pavan et al., 2019). The most common types of semiconductor detectors are the Cadmium Zinc Telluride (CZT or CdZnTe) detectors, high-purity germanium (HPGe) detectors and germanium crystals doped with lithium, Ge(Li).

2.5.2.1 CZT Detectors

As stated in section 1.3, the semiconductor CZT can operate a room temperature and without the need for LN_2. These detectors are currently limited to detection and investigation of low energy photons, for example the Kromek GR1 can be used within the energy range of 30 keV to 3 MeV (Kromek, 2016). The principle of operation described below is based on a revised edition of (Csanád et al., 2012).

Photons are converted into electrons and holes in the CZT detector with the negatively charged electrons and positively charged holes moving towards the oppositely charged electrodes where they are collected. The charge pulse resulting from this process is then detected by a preamplifier, thereby producing a voltage pulse whose height is proportional to the incident energy of the incoming photon. A shaping amplifier converts this charge pulse into a Gaussian pulse by feeding the signal obtained from the preamplifier and amplifies it. A characteristic spectrum of the incoming photons will be generated by the Multi-Channel

Analyzer (MCA) when the amplified signal is finally fed to it. The MCA employs a fast analog-to-digital converter (ADC) to record the incoming pulses from the shaping amplifier. The Kromek GR1 device utilizes pulse-height analysis (PHA) mode of MCA to count pulses based on their amplitude and the number of different amplitudes that are counted depends on the number of channels of the MCA, which is 4096 for the Kromek GR1 detector. This makes it possible to obtain a histogram of channel number against number of counts. This kind of a histogram i.e. a measured pulse height spectrum will be given in our results in the sixth chapter.

Figure 4: Kromek GR1 Spectrometer built with a 1cm^3 CZT detector (Amman, 2017).

2.5.2.2 HPGe Detectors

HPGe detectors can be one of two types: normal or reverse electrode and commonly referred to as "p-type" and "n-type" respectively, denoting the nature of their impurity otherwise known as doping (Shebell, 1999). Due to their relatively low band gap, LN_2 is used to cool the HPGe detectors in order to prevent thermally generated charge carriers to a minimum acceptable level.

An electric field will stretch across the depleted region of the HPGe material under reverse bias and when photons interact within the depleted volume of a detector, charge

carriers (holes and electrons) are generated in proportion to the energy deposited by the incoming photons and then collected by their respective oppositely charged electrodes. This charge is converted into a voltage pulse by an integral charge-sensitive preamplifier, similarly to the CZT detector.

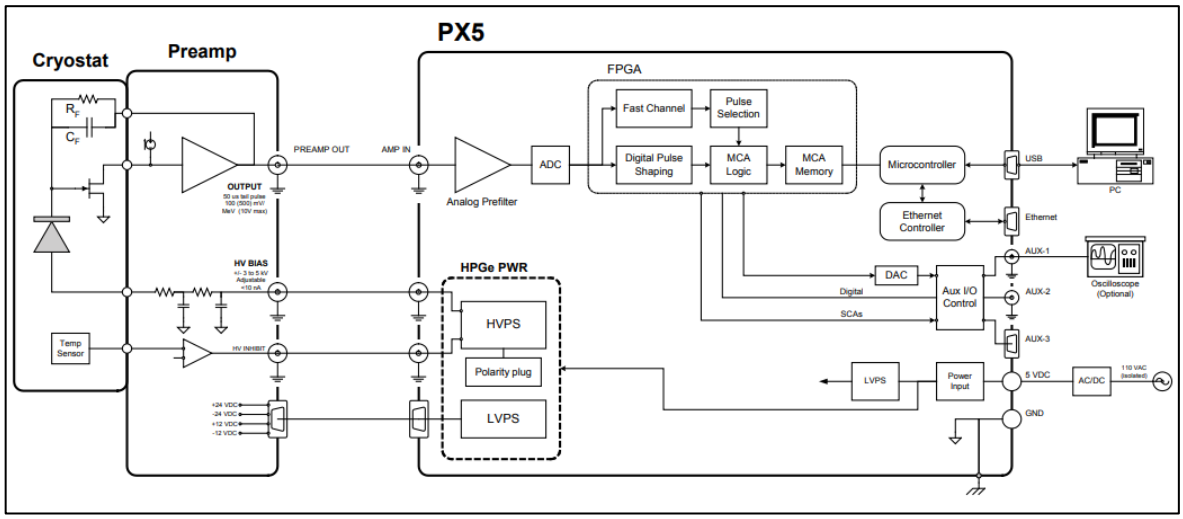

Figure 5: Amptek's PX-5 HPGe detector schematic diagram (Courtesy of Amptek)

3. OBJECTIVES

3.1 General Objectives

The main aim of this thesis is to investigate and provide a comparable analysis on the efficiencies of semi-conductor devices, both with the aid of computer simulations and actual physical laboratory measurements using the Kromek GR1 detector and the HPGe detectors commercially available.

3.2 Specific Objectives

1. Apply acquired knowledge in C++ programming language and GEANT4 in the simulation of a 1 cm3 CZT detector and that of a cylindrical HPGe detector having an outer radius of 2.5cm, an inner radius of 0.2 cm, and a height of 4.2 cm.
2. Record and calculate the efficiencies as a function of photon energy with suitable plots.
3. Take a source known activity and measure its efficiency using a Kromek GR1 detector and then a Measure the absolute activity of a source with the absolute activity measurement (specified in: http://atomfizika.elte.hu/kvml/docs/abs_english.pdf) for both the Kromek and HPGe detectors.
4. Calculate their efficiencies as a function of photon energy by applying physical laws and equations and visualize the results with suitable plots.
5. Compare the results obtained in (4) with the results from the GEANT4 simulations.

4. METHODOLOGY AND RESULTS

4.1 GEANT4 Application: An Overview

GEANT4 is a toolkit used to simulate the passage of particles through matter (S. Agostinelli et al., 2003). GEANT4 implementations are executed using the C++ programming language. As a toolkit, GEANT4 provides extensive libraries applicable in many disciplines but users must define their `main()` programs when building simulation applications. The code implemented for the simulations used in this thesis is provided in Appendices 1-10, while Appendices 11-15 gives the C++ code of the ROOT analysis. Due credits given to (De Simone, 2008) for the introductory guide which was used to explain the very robust GEANT4 in this section.

GEANT4 requires mandatory components in order to function called by their respective classes: G4RunManager, G4VUserDetectorConstruction, G4VPhysicsList, G4VUserPrimaryGeneratorAction, G4UserRunAction, G4UserEventAction, G4UserStackingAction, G4UserTrackingAction, and G4UserSteppingAction. These classes play specific functions in the simulation which this will be illustrated using charts and flow diagrams. The original concept of the charts shown in this section 4.1 was given in (De Simone, 2008) with slight modifications where necessary.

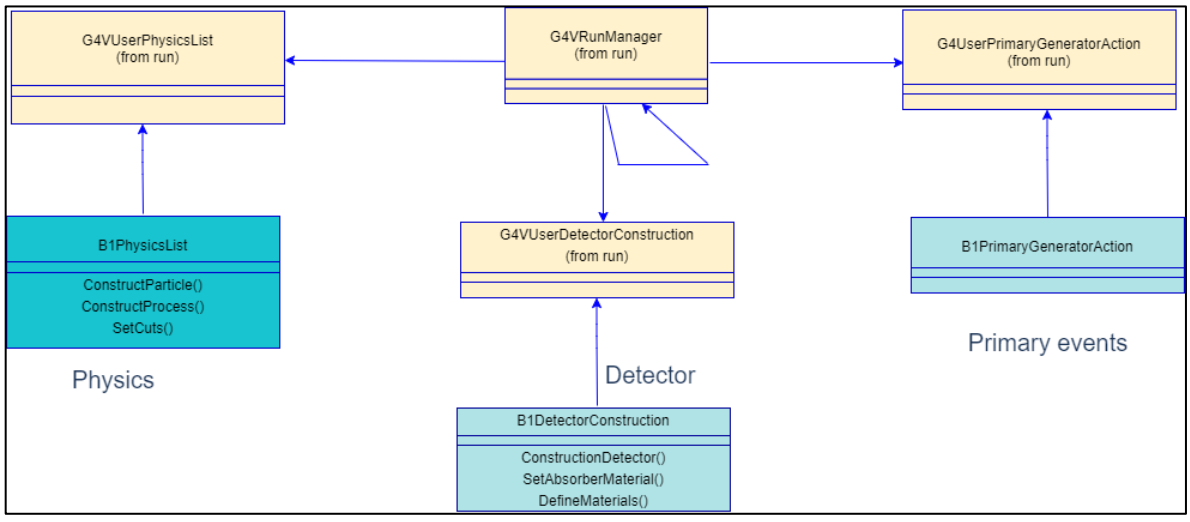

Figure 6: Mandatory User Classes

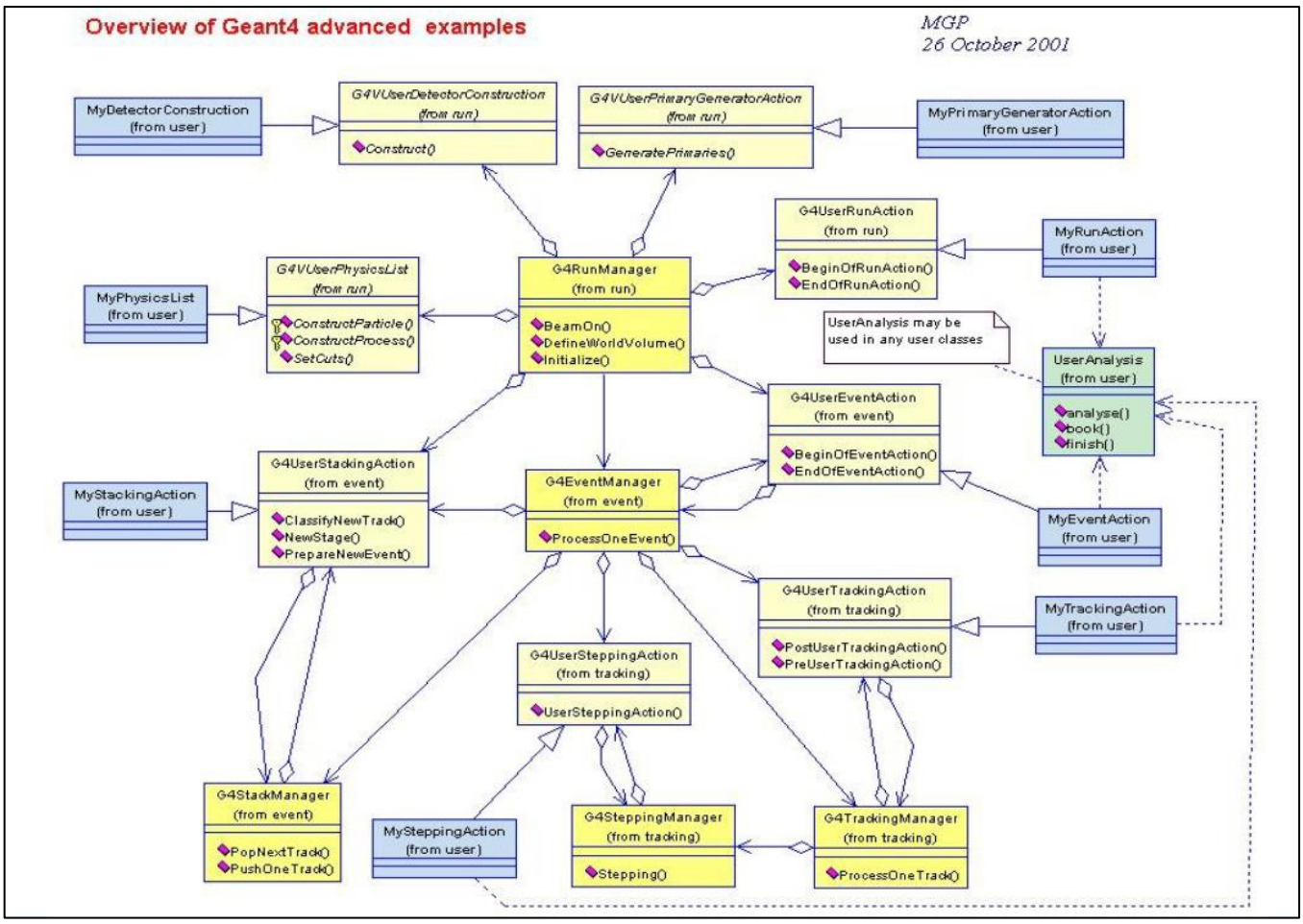

Figure 7: GEANT4 Application Architecture (Simone 2008)

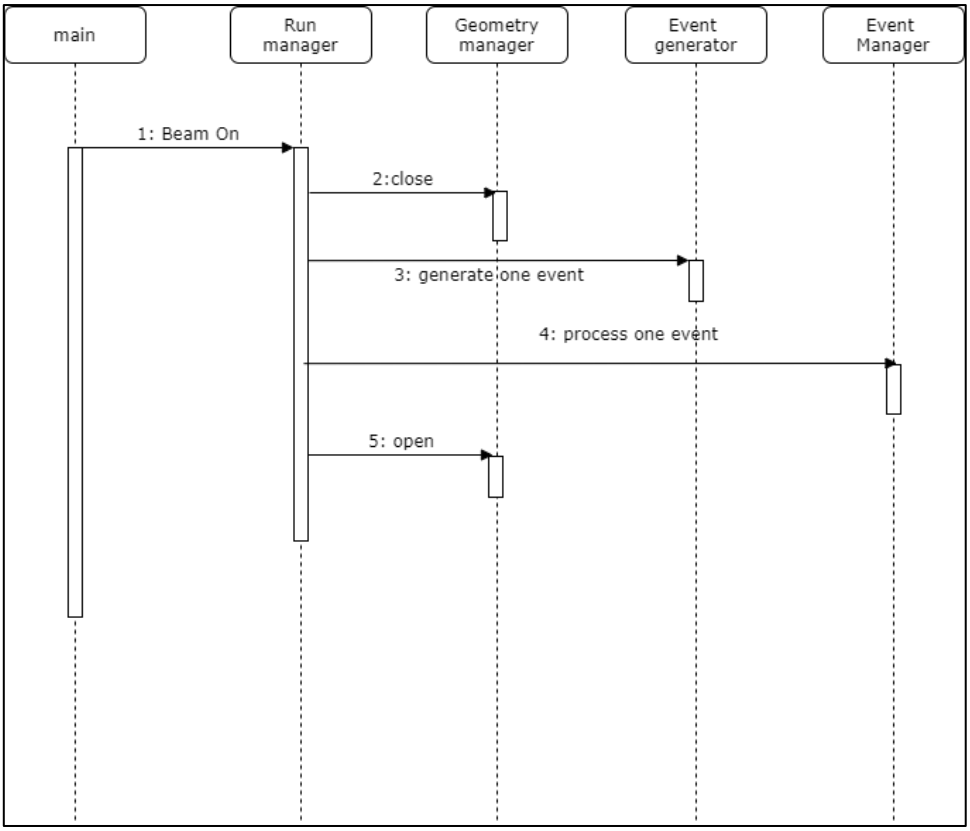

Figure 8: Application flowchart showing mandatory components and the actions they perform.

4.1.1 Detector Construction

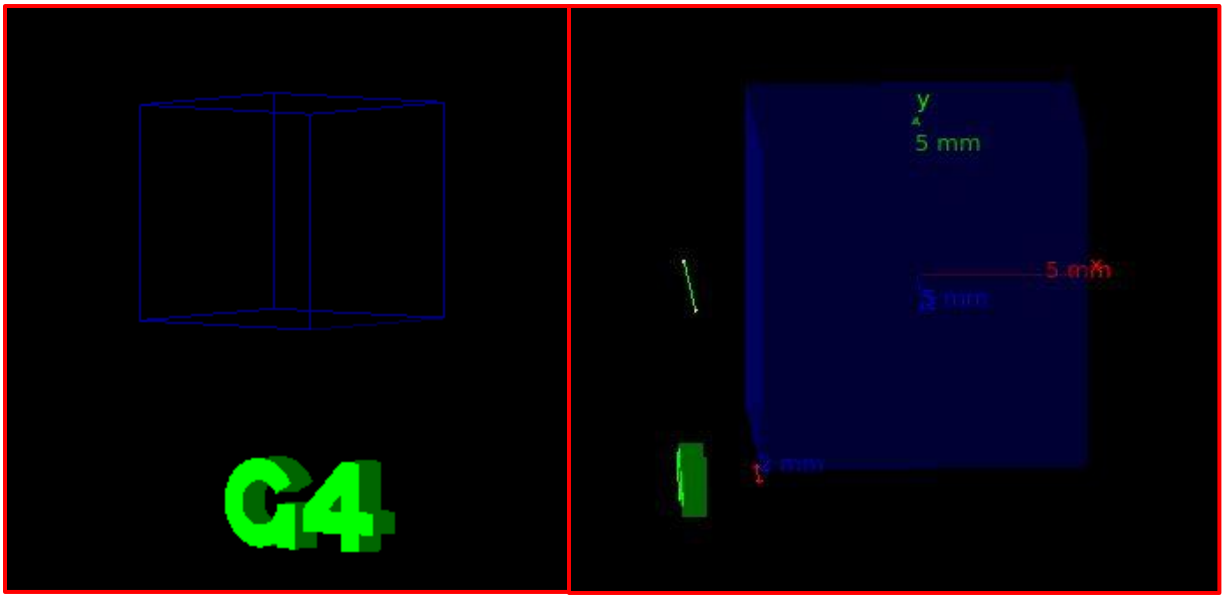

Figure 9: Visualization of the (10x10x10) mm CZT detector

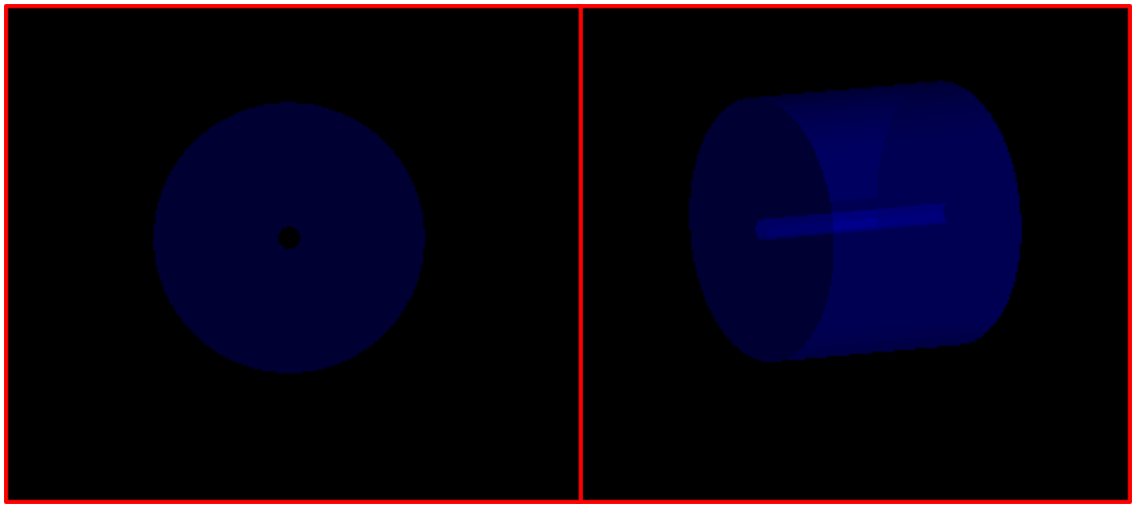

Figure 10: Visualization of the HPGe detector with outer radius 2.5 cm and inner radius 0.2 cm

The run action of the program used for this simulation is shown below.

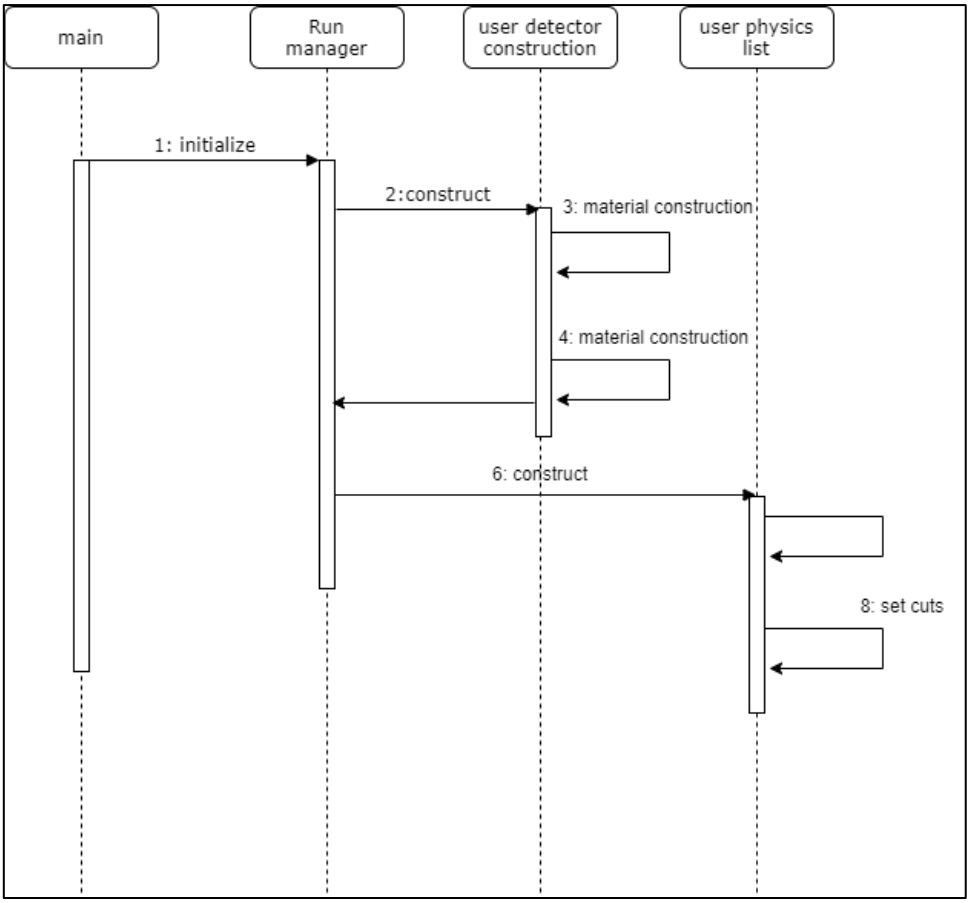

Figure 11: B1RunManager flowchart

4.2 Simulation Results

Table 1 shows the simulations performed for five cases.

Table 1: Cases implemented for simulations.

SN	Detector material	Combined photon energies	Range of combined energies	Medium
1.	CZT	38	25 keV – 3 MeV	Air
2.	CZT	1	661.651 keV	Air
3.	CZT	38	25 keV – 3 MeV	Water
4.	HPGe	38	25 keV – 3 MeV	Air
5.	HPGe	1	661.651 keV	Air

Each case simulation was performed with 100,000 incoming photons and the cross-section of the detector will be visualized after a few strikes by incoming photons and then after the complete strike by 100,000 photons. As stated in section 4.1.2, in order to attain a uniform distribution of the photons, the simulation was performed in such a way to randomize the position where the incoming photons strike the detector volume from a fixed (i.e., nonmoving) radiating particle source. To illustrate this, the trajectory of the incoming photon was recorded and the X-Y distribution of where they strike the detector will be plotted for each case. The histogram of energy deposited on the detectors by the incoming photons for each case simulation will be shown in this chapter.

4.2.1 Result from CZT Simulation

For the first case, the 38 energies of incoming photon energies in keV were: 25, 50, 75, 100, 125, 150, 175, 200, 225, 250, 275, 300, 325, 350, 375, 400, 440, 480, 520, 560, 600, 650, 700, 750, 800, 850, 900, 1000, 1100, 1200, 1300, 1400, 1600, 1800, 2100, 2400, 2700, 3000. This simulation was automated in a single run and in the X-Y distribution chart in figure 13, the total entries is 3,800,000 photons (i.e., 100,000 multiplied by 38). The figures below show how the position of hits on the face of the detectors.

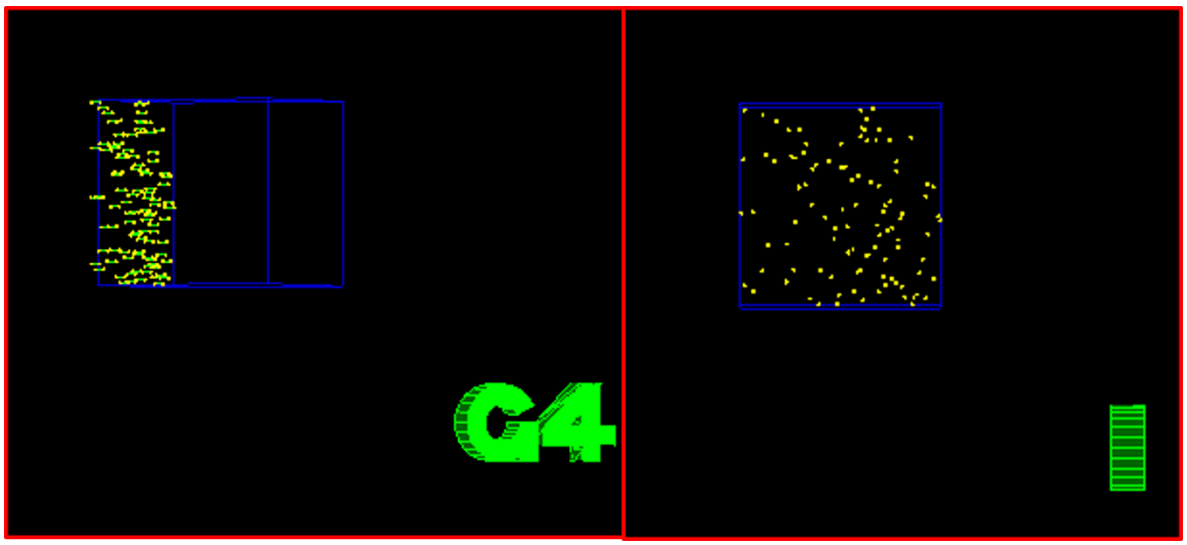

Figure 12:Visualization of incoming photons on the CZT detector during simulation

The positions where the photons were recorded to an output file and was plotted using ROOT in the figures below.

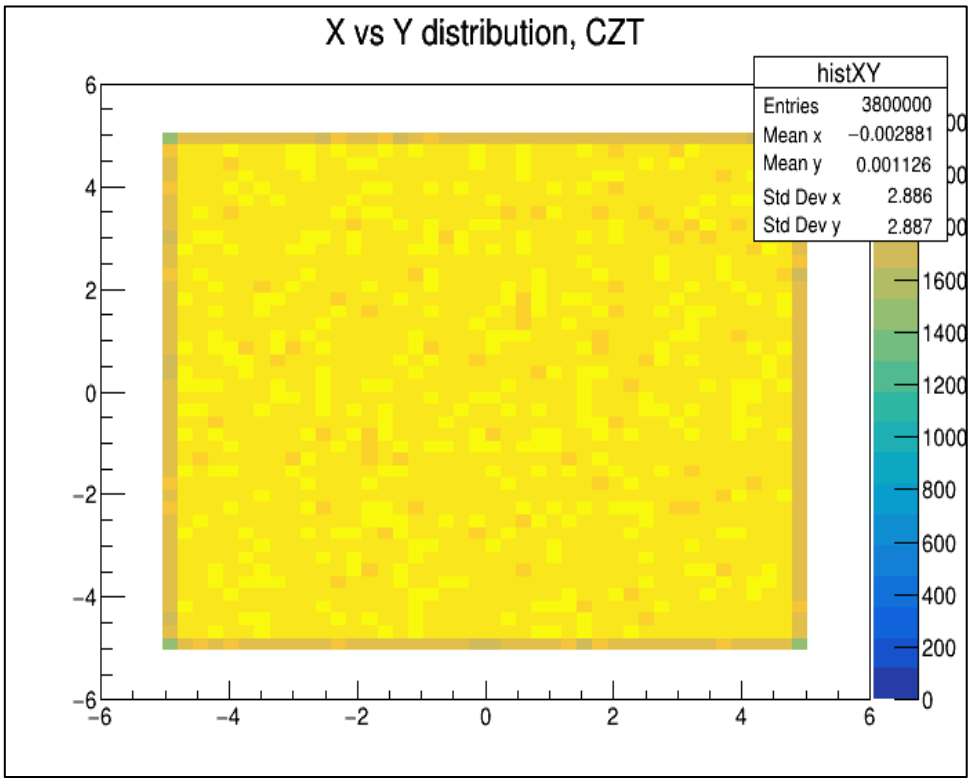

Figure 13: Distribution of incoming photons on the face of the detector.

The energy deposited is plotted in the histograms below:

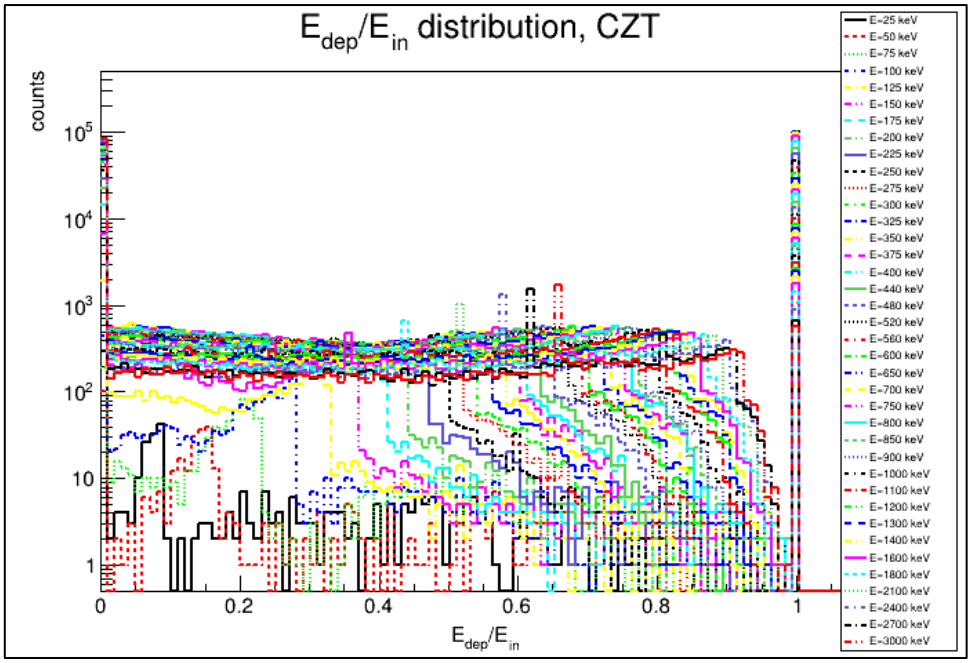

Figure 14: Combined histogram of energy deposition by incoming photons for 38 different energies in air

Let us consider the incoming 100,000 photons for a single energy only and show the randomized point of impact as well as the energy deposition histogram.

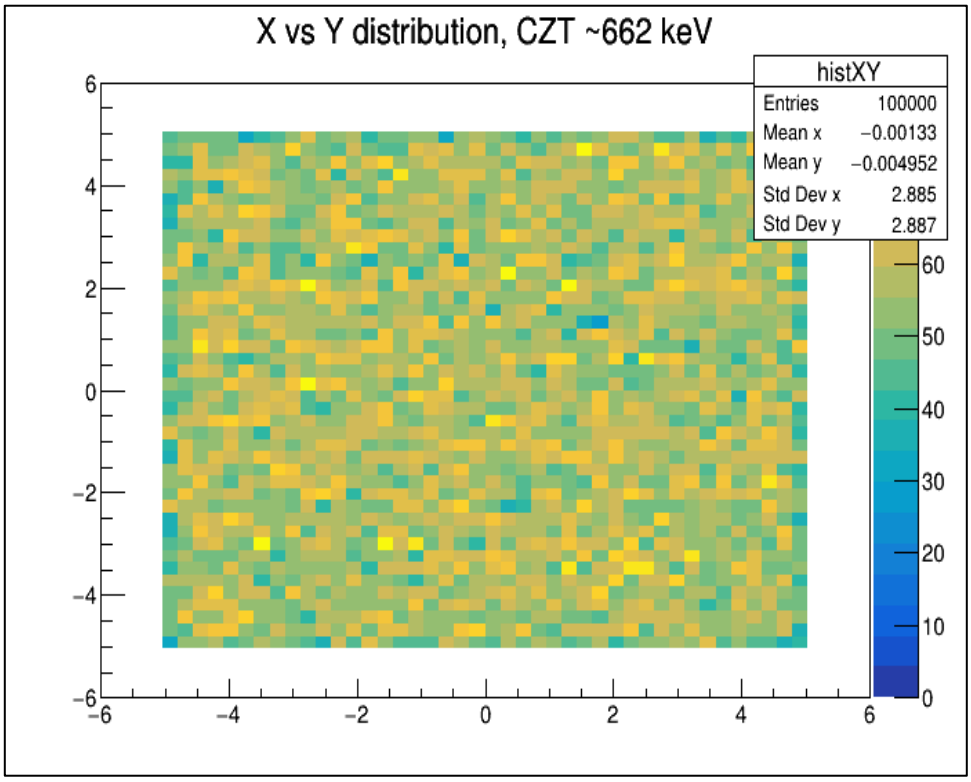

Figure 15: Distribution of incoming ~662 keV photons on the face of the detector.

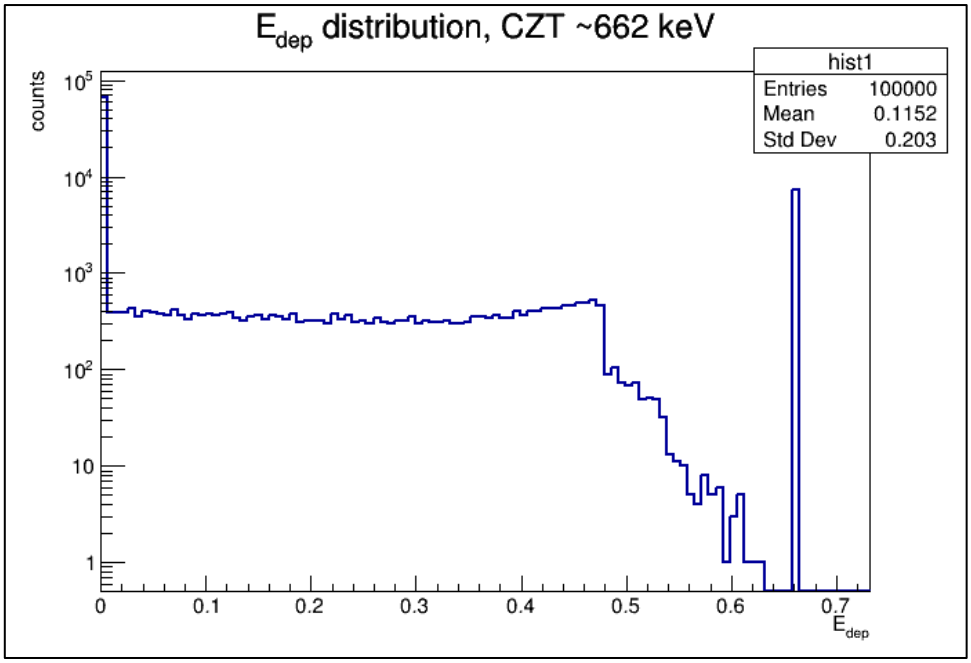

Figure 16: Energy deposition histogram for the ~662 keV photons in air

Now let us investigate the first case when the detector is immersed in water i.e., the third case. The X-Y distribution is like that obtained in the first case; therefore, it is not shown. The figure shows the energy deposition histogram.

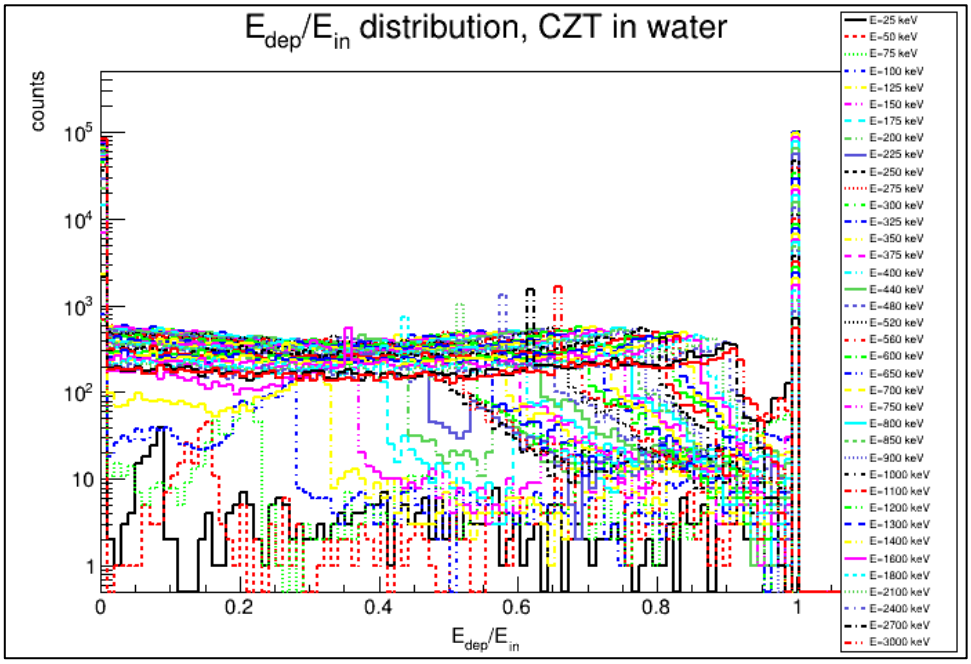

Figure 17: Energy deposition histogram when CZT immersed in water.

4.2.2 Result from HPGe Simulation

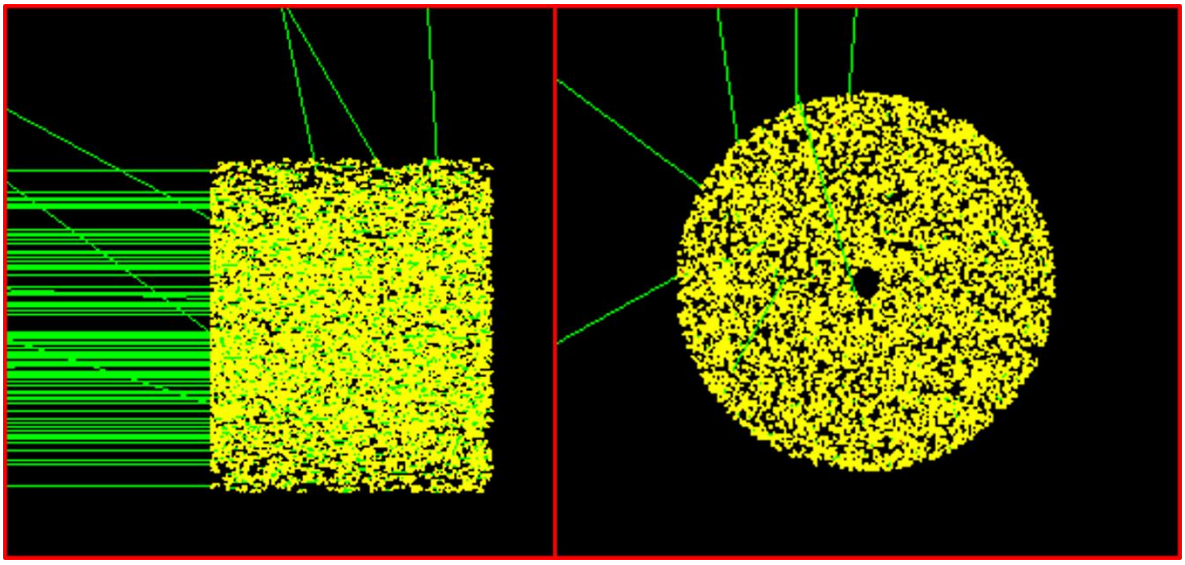

Figure 18: Visualization of the HPGe detector showing incoming photons.

The HPGe simulation was carried out with a similar method as the CZT simulation with only two major differences: the use of a cylindrical high purity germanium material, and the GeneralParticleSource (GPS) class. GPS was used to randomize the trajectory and position where the incoming photons strike along the axis of symmetry of the cylinder in order to optimize the simulation results to account for outer and inner radius in the HPGe detector geometry.

Plots from the fourth case is shown in the figures below.

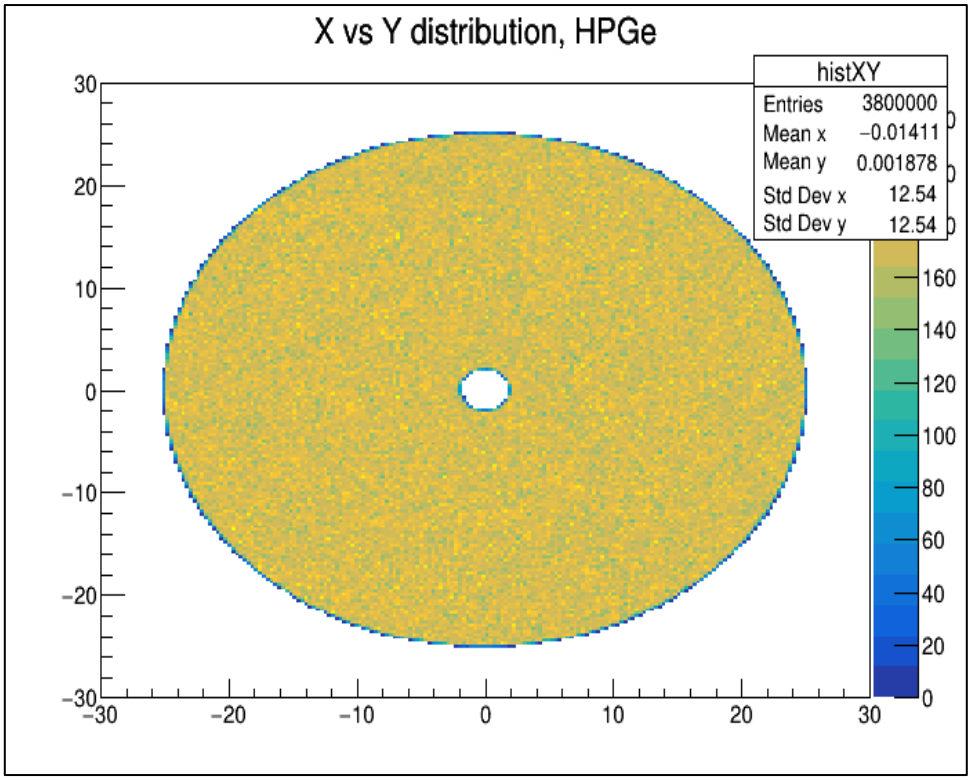

Figure 19: X-Y coordinates of incoming photons

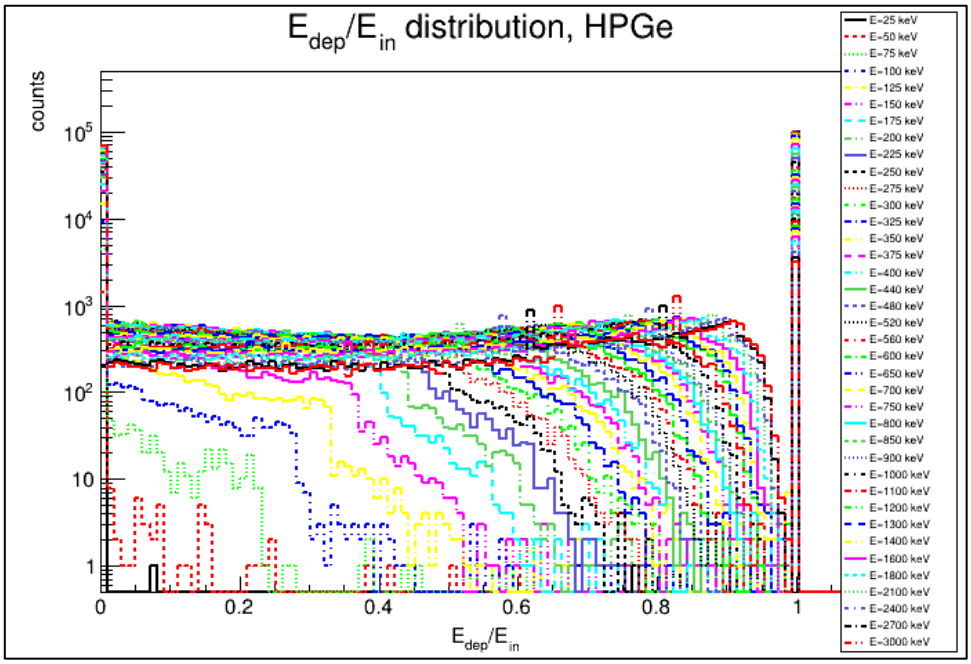

Figure 20: HPGe energy deposition histogram in air

The figures below show the plots from the fifth case. i.e., 661.659 keV photons.

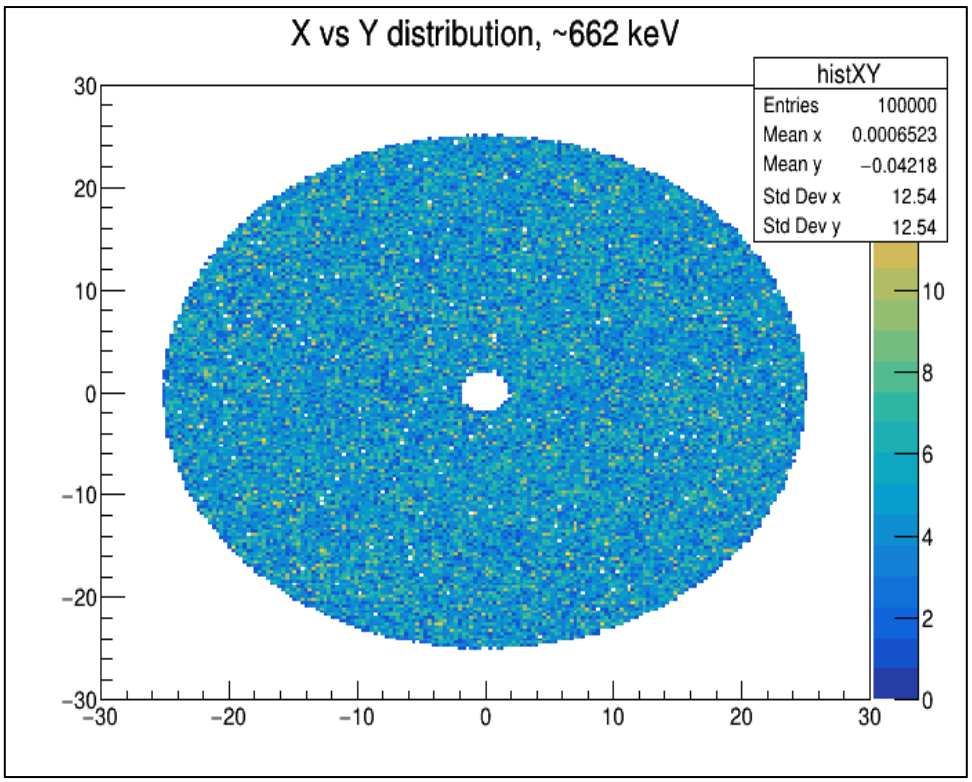

Figure 21: X-Y distribution of incoming photons of ~662 keV

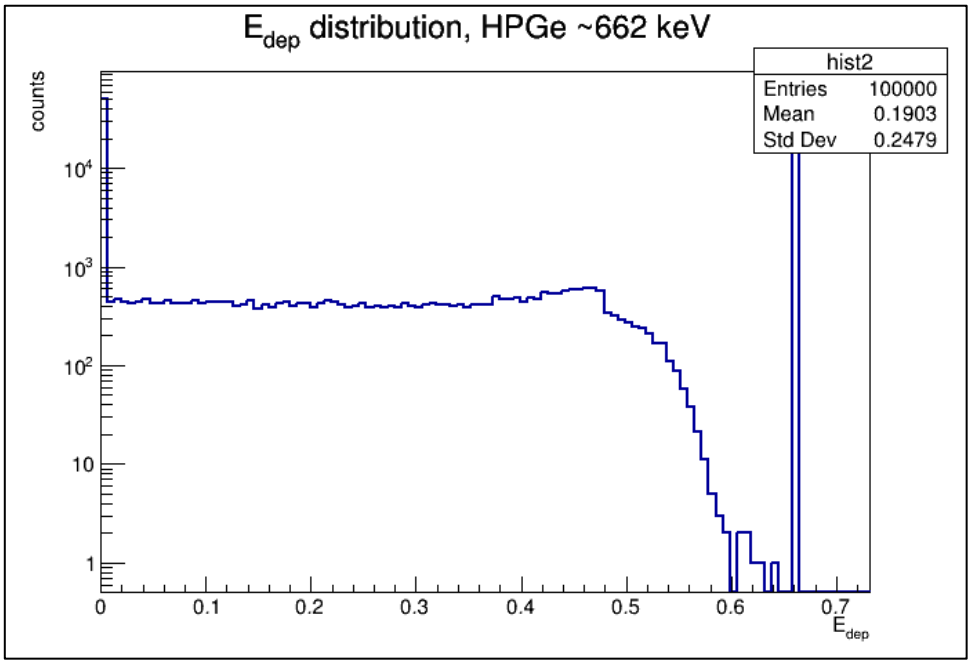

Figure 22: Histogram showing energy deposited against incoming energy of 662 keV in air.

4.3 Laboratory Measurements

Cesium-137 with known activity was used as the radioactive point source for this measurement. The details of the source at the time of measurement are given in Table 2 below.

Table 2: Activity details of our Cs-137 point source

Activity, *A* on July 1, 1963 (21143 days before measurement)	486.55 MBq
Activity, *A* at time of measurement for measurement with Kromek detector on May 20, 2021	128.67 MBq
Activity, *A* at time of measurement for measurement with Canberra HPGe detector on May 27, 2021	121.361 MBq
Half-life	11018.3 days
Decay factor, λ	$2^{-\frac{t}{T}} = 0.264462$
Photon branching ratio	94.36% ± 0.20%
Photon rate	121.47 MBq

4.3.1 Result from Kromek GR1 Measurements

The laboratory setup for this measurement is shown in the figure below.

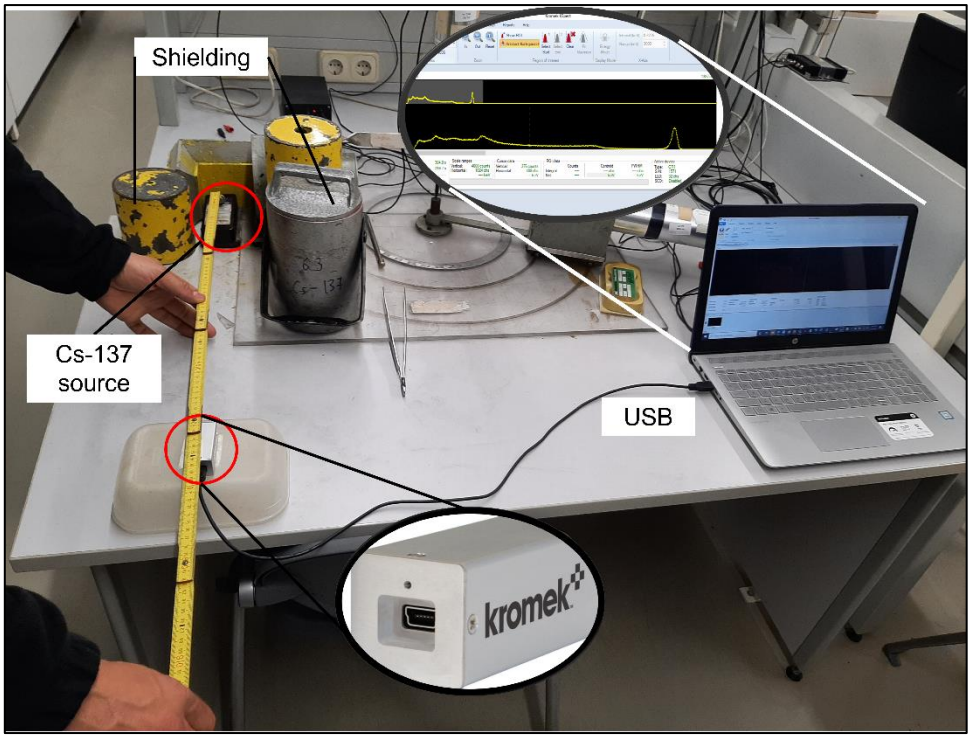

Figure 23: Laboratory setup using Cs-137 as radioactive source 60 cm away from Kromek GR1 detector

In this measurement the Kromek device was connected to the computer via USB. A Cs-137 source of known activity was placed 60 cm away from the detector and the KSpect analyzer was used to view the histogram of energy deposited from the source as shown in the figure below. Measurement time was about 300s.

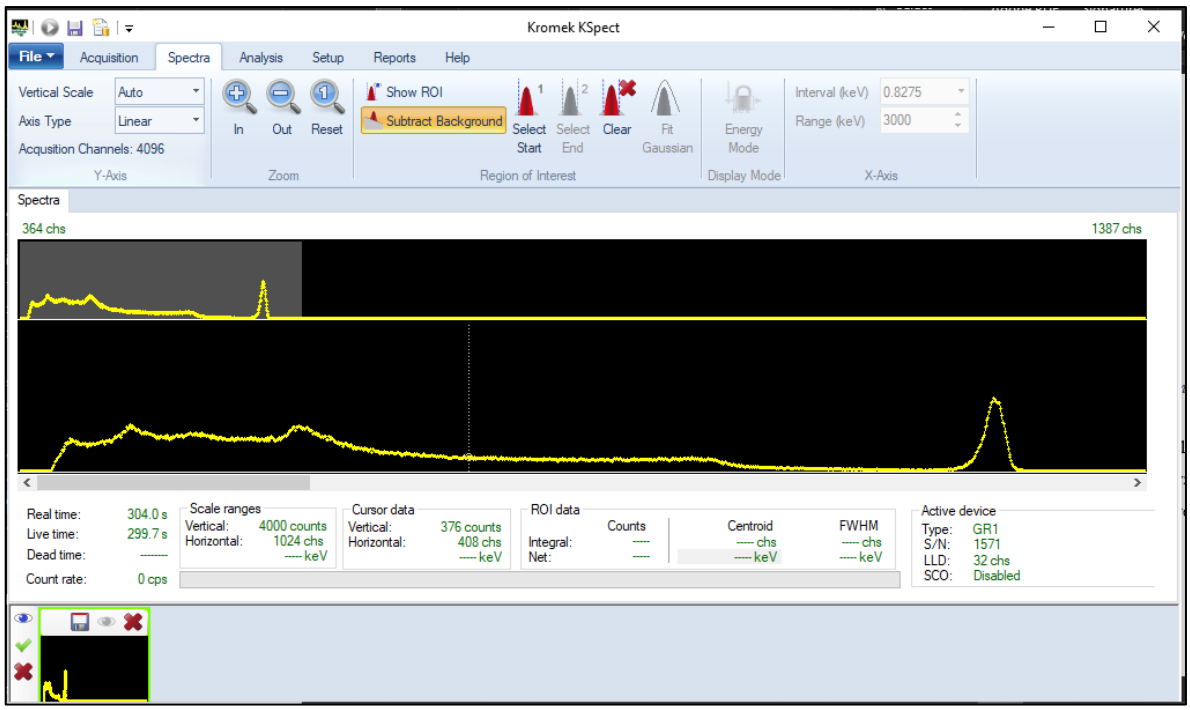

Figure 24: Output from Kromek KSpect Analyzer for Cs-137 source

This laboratory measurement was performed for only two cases: with shielding and without shielding.

4.3.2 Result from Canberra HPGe Measurements

The figure below shows the lab setup for the measurement. The spectrum will be shown in section 4.4.2.

4.4 Efficiency Calculations and Result Comparison

ROOT was used extensively for the physical and mathematical analysis of our results. ROOT which is an objected-oriented program and library written mainly in C++ was developed by CERN. It is a very powerful tool for scientific analysis and visualization of large amounts of data (more details available on https://root.cern/).

4.4.1 Efficiency of simulated detectors

The histograms of energy deposition for the cases in table 1 was plotted with a bin of 110. The total content of this bin indicates the incoming photons on the face of the detectors in each case. Let us consider the simple case with simulation of ~662 keV incoming photons.

In a general sense, the efficiency is given as output divided by input. In this case, to find the efficiency, we use the area under the actual full energy peak (~662 keV) divided by the area under the spectrum (i.e., with respect to the total detected energies). This is achieved using integration, thus mathematically:

$$\epsilon = \frac{\int(photons\ detected\ at\ full\ energy\ peak, 661.659\ keV)}{\int(total\ detected\ photons\ at\ all\ energies)} \tag{24}$$

The histograms of energy deposition were plotted with a bin of 110 and the full energy peak lies between bins 99 and 101. Therefore, the translation of the computation performed in the ROOT code (see Appendix 12) is thus:

$$\epsilon = \frac{\int(bins\ 99 - 101)}{\int(bins\ 1 - 110)} \tag{25}$$

The error was computed using:

$$\epsilon_{error} = \epsilon \times \sqrt{\frac{1}{(full\ energy\ peak\ of\ 661.659\ keV)} + \frac{1}{\int(total\ detected\ energies)}} \tag{26}$$

The result of the ROOT computation is:

Table 3: Efficiency of simulated detectors at 661.659 keV

Simulation Case no. (from table 1)	Detector material	Efficiency
3	CZT	*7.24% ± 0.09%*
5	HPGe	*14.76% ± 0.13%*

It is important to highlight once again that these values were arrived at based on the simulations.

For the simulation cases 1,3 and 4 with different energies of the photons combined in a single histogram, we apply the following formula below to obtain the efficiency of the CZT detector in air and water medium in simulation cases 1 and 2, respectively.

$$\epsilon(E) = a \cdot c\left(\frac{E}{E_0}\right)^{-b}\left\{1 - \exp\left[-\frac{1}{c}\left(\frac{E}{E_0}\right)\right]^{b}\right\} \cdot \left(1 + d \cdot \frac{E}{E_0}\right) \tag{27}$$

For the HPGe detector in simulation case 4, we use:

$$\epsilon(E) = a \cdot c\left(\frac{E}{E_0}\right)^{-b}\left\{1 - \exp\left[-\frac{1}{c}\left(\frac{E}{E_0}\right)\right]^{b}\right\} \cdot \left(1 + d \cdot \left(\frac{E}{E_0}\right)^{3/4}\right) \qquad (28)$$

These formulas were found by a trial-and-error type of method, based on the apparent power-law behavior for large energies (i.e., linear on a log-log plot) and a saturation for small energies. The factor $\left(\frac{E}{E_0}\right)^{-b}$ is responsible for the power-law tail, and to create a little correction for the largest energies we multiply by the factor $\left(1 + d \cdot \frac{E}{E_0}\right)$ for the CZT detector and $\left(1 + d \cdot \left(\frac{E}{E_0}\right)^{3/4}\right)$ for the HPGe detector. The exponential part creates the saturation, using the fact that $1 - e^{-x} \cong 1$ for small *x* values.

This formula maximum exceeds one which is not meaningful for an efficiency, the minimum value of one and the result of the formula was taken. This way a number that is smaller than (or equal to) one was obtained. The formula was constructed in such a way that for small energies, it converges to a constant, *a*. However, since there may still be a small and broad maximum at small energies, even exceeding one, the above-mentioned maximization was utilized.

The figure below shows the plot of the incoming energy photons against efficiency for cases 1, 2, and 4, respectively. The efficiency value for each energy was calculated in the same was as in equation (24) above, however the fit (i.e., the lines connecting the efficiency values) was computed using the formulae in equations (27) and (28) for CZT and HPGe detectors, respectively. The fit parameters a, b, c, and in the equations was obtained using ROOT and specified in the table below. Note that E_0 was fixed at 1 keV to ensure correct base unit in all cases.

In table 4, chi^2 is the goodness of fit calculated as:

$$x^2 = \sum_i \frac{(x_i - y_i(a))^2}{{e_i}^2} \qquad (29)$$

where x_i are the data points, $y_i(a)$ are the calculated function values with given parameters a, and e_i are the data uncertainties.

Table 4: Fit parameters for simulation cases 1, 2 and 5.

Fit Parameter	CZT	CZT in water	HPGe
a	*0.927 ± 0.006*	*0.903 ± 0.006*	*0.816 ± 0.013*
b	*2.469 ± 0.006*	*2.480 ± 0.006*	*1.872 ± 0.007*
c	*(239 ± 7) · 10^3*	*(250 ± 7) · 10^3*	*(5.721 ± 0.12) · 10^3*
d	*(3.146 ± 0.10) · 10^{-3}*	*(3.38 ± 0.11) · 10^{-3}*	*(7.521 ± 0.465) · 10^{-3}*
E_0	1 keV (fixed)	1 keV (fixed)	1 keV (fixed)
chi^2	*108*	*153*	*147*

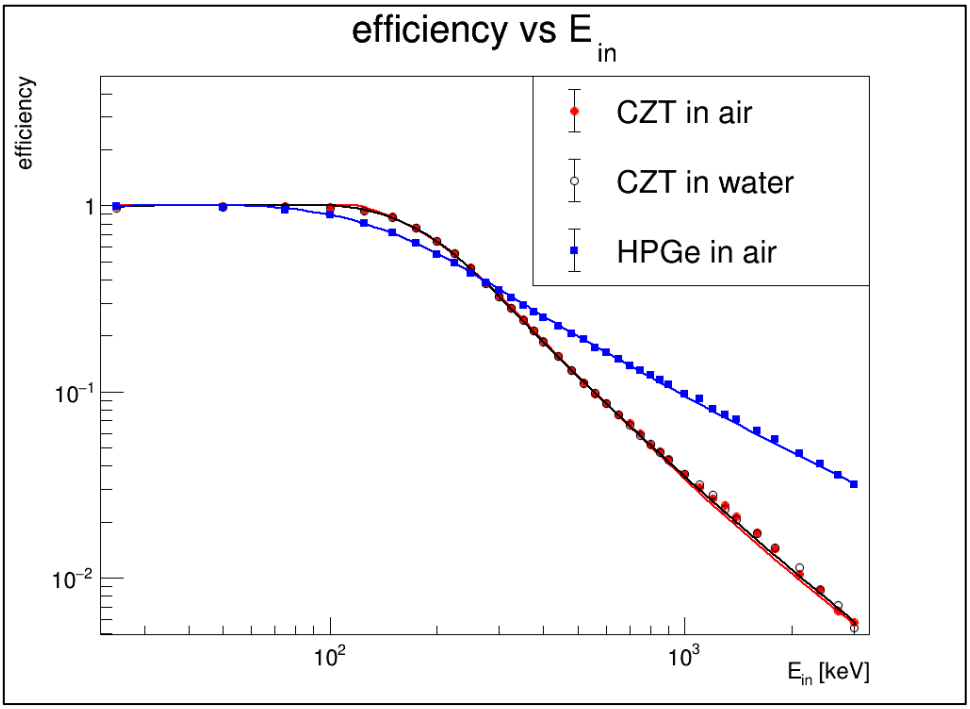

Figure 25: Efficiency plots of simulation cases with combined energies

4.4.2 Efficiency of Kromek GR1 and Canberra HPGe

Recall from table 2 at time of measurement activity, *A* is *128.67 MBq* but it was *486.55 MBq* at point of collection on July 1, 1963.

The branching ratio for the sample is *94.36% ± 0.20%* which indicates the percentage of particles that will decay with respect to the total decaying particles. Therefore, the activity becomes:

$$A_{true} = 128.67 \times 10^6 \times 0.9436 = 121.41 \cdot 10^6\ s^{-1} \quad (30)$$

Taking Cs-137 as a point source, we can illustrate it as in the figure below.

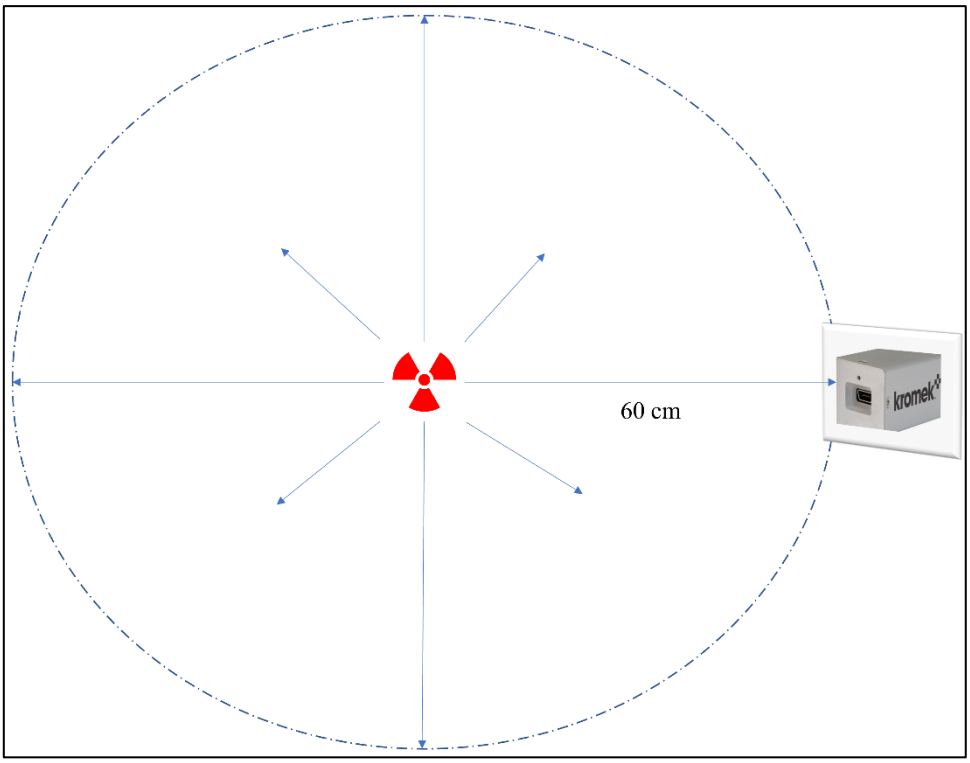

Figure 26: Cs-137 as a point source radiating equally in all directions around a sphere.

To find the number of particles (N_{true}) absorbed at the *1* cm^2 cross-section of the detector placed at 60 *cm* from the radius of the sphere, we perform the following:

$$N_{true} = 121.4 \cdot 10^6 \times \frac{1\ cm^2}{(4\pi \times 60^2)\ cm^2} = 2683.81\ s^{-1} \quad (31)$$

The KSpect data was extracted to a text file in order to use ROOT to plot a Gaussian fit around the full energy peak as shown below.

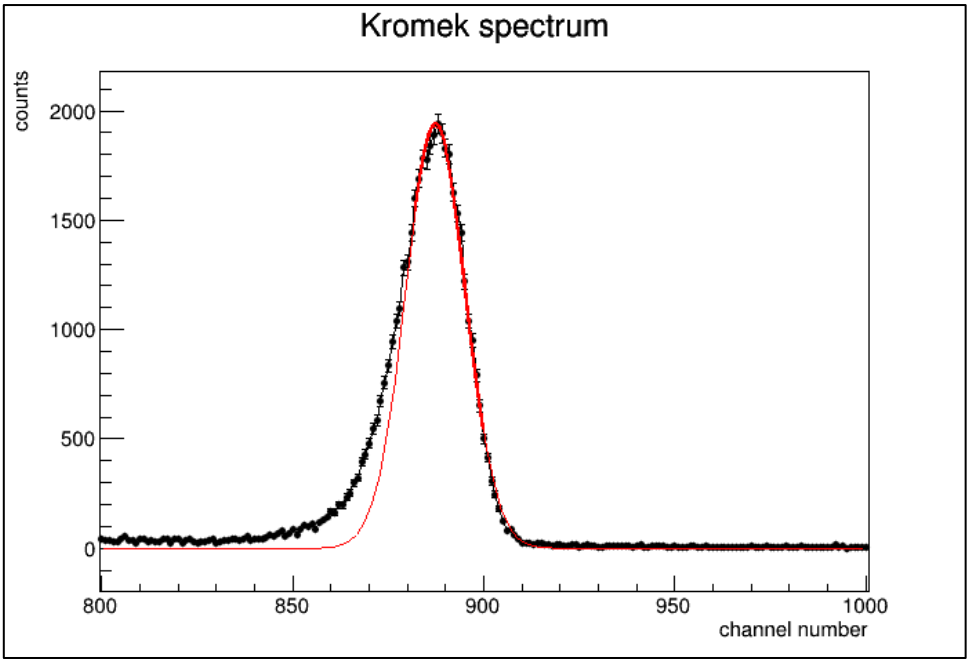

Figure 27: Kromek spectrum full energy peak with Gaussian fit

The Gaussian fit function in ROOT is given as:

$$f(x) = p_0 \cdot \exp\left(-0.5 \cdot \frac{(x-c)^2}{2\sigma^2}\right) \tag{32}$$

Where p_0 is the amplitude of the peak, c is the position of the centroid, and σ is the standard deviation which determines the width of the curve (or fit in this case) and it is proportional to the full width at half maximum (FWHM). The integration of this function will give the area under the curve which corresponds to the number of particles. Thus,

$$\int f(x) \cdot dx = p_0 \cdot c \cdot \sqrt{2\pi} \tag{33}$$

From the ROOT computation we obtained $c = 7.87 \pm 0.12$, and $p_0 = 1940.37 \pm 14.77$. Substituting the values obtained from the fit into (32) we obtain:

$$A_{meas.} = \sqrt{2\pi} \cdot 7.87 \cdot 1940.37 = 38.27 \times 10^3\ s^{-1} \tag{34}$$

To obtain $N_{meas.}$ we divide this value by 300s which is the time duration for the measurement. Thus,

$$N_{meas.} = \frac{38.27 \times 10^3}{300} = 127.57\ s^{-1} \tag{35}$$

$$\in = \frac{\Delta N_{meas.}}{\Delta N_{true}} = \frac{127.57}{2683.81} = 0.0475 = 4.75\% \quad (36)$$

The propagation of error was calculated taking into consideration the uncertainties of the branching ratio, distance (which was squared), and the uncertainty of values used to obtain N_{meas}. By applying the propagation of error formula, we can calculate the relative error for N_{meas}, thus:

$$\sigma_{\in} = \sqrt{\left(\frac{0.02}{0.9436}\right)^2 + \left(\frac{0.5}{60}\right)^2 + \left(\frac{0.5}{60}\right)^2 + \left(\frac{0.12}{7.87}\right)^2 + \left(\frac{14.77}{1940.37}\right)^2} = 0.0296 \quad (37)$$

For the full uncertainty, we use:

$$4.75\% \times 0.0296 = 0.14\% \quad (38)$$

Hence, our efficiency for the Kromek device (taking full uncertainty into consideration) is $4.75\% \pm 0.14\%$.

The computation for HPGe was performed using the same procedure (but in Excel for the sake of ease) to obtain an efficiency of $3.64\% \pm 7.28\%$.

5. DISCUSSIONS

The results obtained in section 4 confirms that the HPGe detectors have a higher efficiency compared to the CZT detector making it more suitable for higher energy photon detection and measurements. Both detectors have higher efficiencies at lower energies are suitable for low energy photon detection as seen from the efficiency plots in section four.

For the water case for the CZT detector, in the given 0.5 mm water layer, gamma intensity reduces to roughly 97% for 25 keV photons, 99% for 50-100 keV photons, and increases slowly to 99.8% for 3 MeV photons. This distortion is barely visible above 100 keV, but for the lowest energy points, it causes an observable decrease of the efficiency when water was used in the simulation in between the detector and the photons (M.J Berger, 1998).

The Kromek GR1 CZT detector which utilizes differential measurement of induced charge is a good improvement from CZT detectors obtainable in the past. According to (Amman, 2017), “this differential measurement of the induced charge solves the inherent charge transport problems of CdZnTe by eliminating the effects of poor hole transport and electron trapping, and thereby enables relatively large detectors to be produced with good spectral performance.”

6. CONCLUSION

In this thesis work we have compared the efficiencies of two kinds of detectors – the Kromek GR1 and the Canberra HPge detectors. The Kromek CZT detector is an innovation on gamma spectroscopy, although it can be greatly improved. The HPGe has a higher efficiency and it is suitable where higher energy photons need to be monitored.

Advancements in nuclear research has given rise to applications of radioactivity in many areas. As these applications of radioactivity continues to grow, the importance of advanced, accurate, and reliable in-situ measurement techniques cannot be overemphasized. Innovative technologies have made it possible to fabricate portable gamma ray detectors at a commercial level and this thesis explores the practicability of such detectors.

The Kromek GR1 is a good choice for preliminary investigations but due to its low resolution, it *may* not provide results required for in-depth analysis and investigations of samples.

REFERENCES

1. Amman M., Lee J., Luke P., Sturm B.

   Ultra-Compact and Low-Power, High-Resolution Spectrometer (Coplanar Grid Spectrometer)

   Lawrence Berkeley National Laboratory, 2017

2. Bagshaw, M., & Illig, P. (2019).

   The Aircraft Cabin Environment. Travel Medicine

   Travel Medicine (Fourth Edition), Elsevier, 2019, Pages 429-436, ISBN 9780323546966,

   https://doi.org/10.1016/B978-0-323-54696-6.00047-1

3. Ball, D.W and Key J.A.

   Introductory Chemistry - 1st Canadian Edition

   BCcampus, 2014, ISBN 13: 9781774200032

   https://opentextbc.ca/introductorychemistry/

4. Bohr N.

   On the Constitution of Atoms and Molecules

   Philosophical Magazine, Series 6, Vol. 26, July 1913, pp 1-25

5. Chadwick J.

   The Neutron and its Properties

   Nobel Lecture, December 12, 1935

6. Csanád M., Horváth Á, Horváth G.,

   Environmental Physics Methods Laboratory Practices,

   Eötvös Loránd University Faculty of Science, 2012, ISBN 978-963-279-551-5.

   http://atomfizika.elte.hu/kornyfizlab/docs/Environmental_physics.pdf

7. De Simone A.

   Introduction to Geant4

   Uni Freiburg, 2008

   http://people.roma2.infn.it/~morselli/CorsoToV/G4tutorial_shortDiSimone.pdf

8. E. Fonollosa, A. Peñalver, F. Borrull, C. Aguilar

Radon in spring waters in the south of Catalonia

Journal of Environmental Radioactivity, 151 (2016), pp. 275-281

https://doi.org/10.1016/j.jenvrad.2015.10.019.

9. Environmental Protection Agency, EPA

Natural Radioactivity in Food

https://www.epa.gov/radtown/natural-radioactivity-food

Date published: June 14, 2019, Date accessed: May 26, 2021

10. Evans R.D.

The Atomic Nucleus

McGraw, 1955

11. Gabor T. Herman,

Fundamentals of computerized tomography: image reconstruction from projections, 2nd edition

ISBN 978-1-85233-617-2.

Springer-Verlag London, ©2009.

12. International Atomic Energy Agency, IAEA

Natural and Induced Radioactivity in Food

IAEA, VIENNA, 2002, IAEA-TECDOC-1287, ISSN 1011–4289

https://www-pub.iaea.org/MTCD/Publications/PDF/te_1287_prn.pdf

13. International Atomic Energy Agency, IAEA

Radiation Technology: The industrial revolution behind the scenes.

IAEA BULLETIN; The flagship publication of the IAEA| Editor: Miklos Gaspar | March 2017

https://www.iaea.org/sites/default/files/bull581mar2017.pdf

14. K. Kovler, H. Friedmann, B. Michalik, W. Schroeyers, A. Tsapalov, S. Antropov, T. Bituh, D. Nicolaides,

3 - Basic aspects of natural radioactivity,

Naturally Occurring Radioactive Materials in Construction, Woodhead Publishing, 2017, Pages 13-36, ISBN 9780081020098,

https://doi.org/10.1016/B978-0-08-102009-8.00003-7.

15. Kromek Group

GR1-A® and GR1® the World's Smallest and Highest Resolution Room Temperature Gamma-Ray Spectrometers

Kromek Group, 2016

https://www.kromek.com/images/products/GR1USLRev12.pdf

16. Loveland W., Morrissey D.J., Seaborg G.T.

Modern Nuclear Chemistry

Wiley, 2005 ISBN-10 0-471-11532-0

17. M.J. Berger, J.H. Hubbell, S.M. Seltzer, J. Chang, J.S. Coursey, R. Sukumar, D.S. Zucker, and K. Olsen

NIST Standard Reference Database 8 (XGAM)

NIST, PML, Radiation Physics Division

18. N.A. Beresford, S. Fesenko, A. Konoplev, L. Skuterud, J.T. Smith, G. Voigt,

Thirty years after the Chernobyl accident: What lessons have we learnt?,

Journal of Environmental Radioactivity, Volume 157, 2016, Pages 77-89, ISSN 0265-931X.

https://doi.org/10.1016/j.jenvrad.2016.02.003.

19. Nancy Vogeltanz-Holma, Gary G. Schwartz

Radon and lung cancer: What does the public really know?

Journal of Environmental Radioactivity, Volume 192, 2018, Pages 26-31, ISSN 0265-931X

https://doi.org/10.1016/j.jenvrad.2018.05.017.

20. National Research Council (U.S.), Committee on Health Risks of Exposure to Radon

Health effects of exposure to radon

National Academy Press; BEIR VI. Washington, D.C. 1999.

https://www.nap.edu/download/5499

21. Pavan M., Raja V, Barron Andrew R.

Physical Methods in Chemistry and Nano Science

OpenStax CNX. Jan 20, 2019

http://cnx.org/contents/ba27839d-5042-4a40-afcf-c0e6e39fb454@25.2.

22. Rajamanickam Baskar, Kuo Ann Lee1, Richard Yeo1 and Kheng-Wei Yeoh

Cancer and Radiation Therapy: Current Advances and Future Directions

International Journal of Medical Sciences, 2012; 9(3):193-199. doi: 10.7150/ijms.3635

http://dx.doi.org/10.7150/ijms.3635

23. Robert P. Kirshner,

The Earth's Element.

Scientific American, 2014.

http://dx.doi.org/10.1038/scientificamerican1094-58

24. Rutherford E.,

The Scattering of α and β Particles by Matter and the Structure of the Atom

Philosophical Magazine, Series 6, vol. 21, May 1911, p. 669-688

25. S. Agostinelli, J. Allison, K. Amako, J. Apostolakis, H. Araujo, P. Arce, M. Asai, D. Axen, S. Banerjee, G. Barrand, F. Behner, L. Bellagamba, J. Boudreau, et al.

Geant4—a simulation toolkit,

Nuclear Instruments and Methods in Physics Research Section A: Accelerators, Spectrometers, Detectors and Associated Equipment, Volume 506, Issue 3, 2003, Pages 250-303, ISSN 0168-9002,

https://doi.org/10.1016/S0168-9002(03)01368-8.

26. Samet, Jonathan M.,

Radiation and cancer risk: a continuing challenge for epidemiologists,

Environmental Health Journal, 2011,

https://doi.org/10.1186/1476-069X-10-S1-S4

27. Seegenschmiedt, M. H., Micke, O., Muecke, R., & German Cooperative Group on Radiotherapy for Non-malignant Diseases (GCG-BD) (2015).

Radiotherapy for non-malignant disorders: state of the art and update of the evidence-based practice guidelines.

The British journal of radiology, 2015, 88(1051), 20150080.

https://doi.org/10.1259/bjr.20150080

28. Shebell, P.

Portable gamma-ray spectrometers and spectrometry systems.
International Atomic Energy Agency (IAEA), IAEA TECDOC--1121, 1999
https://inis.iaea.org/collection/NCLCollectionStore/_Public/30/060/30060366.pdf?r=1

29. Spurný F.,
Radiation doses at high altitudes and during space flights,
Radiation Physics and Chemistry,
Volume 61, Issues 3–6, 2001, Pages 301-307, ISSN 0969-806X,
https://doi.org/10.1016/S0969-806X(01)00253-5.

30. United Nations Scientific Committee on the Effects of Atomic Radiation,
Sources and Effects of Ionizing radiation,
Report to the General Assembly with Scientific Annexes, UNSCEAR 2008.
https://www.unscear.org/docs/publications/2008/UNSCEAR_2008_Report_Vol.I.pdf

31. U.S. Department of Energy
Series on Nuclear Energy
Office of Nuclear Energy, Science, and Technology 2002, DOE/NE-0088
Retrieved May 26, 2021
https://www.energy.gov/sites/default/files/The%20History%20of%20Nuclear%20Energy_0.pdf

32. V. Moreno, J. Bach, C. Baixeras, L. Font
Radon levels in groundwaters and natural radioactivity in soils of the volcanic region of La Garrotxa
Spain. J. Environ. Radioact., 128 (2014), pp. 1-8

33. Viktor Jobbágy, Timotheos Altzitzoglou, Petya Malo, Vesa Tanner, Mikael Hult,
A brief overview on radon measurements in drinking water,
Journal of Environmental Radioactivity, Volume 173, 2017, Pages 18-24,
https://doi.org/10.1016/j.jenvrad.2016.09.019.

34. World Nuclear Association
Nuclear Power Today

World Nuclear Association website article, Updated March 2021, Date accessed: May 26, 2021
https://www.world-nuclear.org/information-library/current-and-future-generation/nuclear-power-in-the-world-today.aspx#:~:text=Around%2010%25%20of%20the%20world's,from%202563%20TWh%20in%202018.

APPENDICES

Appendix 1: B1ActionInitialization.cc

```
//
// ********************************************************************
// * License and Disclaimer                                           *
// *                                                                  *
// * The  Geant4 software  is  copyright of the Copyright Holders  of *
// * the Geant4 Collaboration.  It is provided  under  the terms  and *
// * conditions of the Geant4 Software License,  included in the file *
// * LICENSE and available at  http://cern.ch/geant4/license .  These *
// * include a list of copyright holders.                             *
// *                                                                  *
// * Neither the authors of this software system, nor their employing *
// * institutes,nor the agencies providing financial support for this *
// * work  make  any representation or  warranty, express or implied, *
// * regarding  this  software system or assume any liability for its *
// * use.  Please see the license in the file  LICENSE  and URL above *
// * for the full disclaimer and the limitation of liability.         *
// *                                                                  *
// * This code  implementation is the result of  the  scientific and *
// * technical work of the GEANT4 collaboration.                      *
// * By using,  copying,  modifying or  distributing the software (or *
// * any work based  on the software)  you  agree  to acknowledge its *
// * use  in  resulting  scientific  publications,  and indicate your *
// * acceptance of all terms of the Geant4 Software license.          *
// ********************************************************************
//
/// \file B1ActionInitialization.cc
/// \brief Implementation of the B1ActionInitialization class

#include "B1ActionInitialization.hh"
#include "B1PrimaryGeneratorAction.hh"
#include "B1RunAction.hh"
#include "B1EventAction.hh"
#include "B1SteppingAction.hh"

//....oooOOOOOooo........oooOOOOOooo........oooOOOOOooo........oooOOOOOooo......

B1ActionInitialization::B1ActionInitialization()
 : G4VUserActionInitialization()
{}
//....oooOOOOOooo........oooOOOOOooo........oooOOOOOooo........oooOOOOOooo......

B1ActionInitialization::~B1ActionInitialization()
{}
//....oooOOOOOooo........oooOOOOOooo........oooOOOOOooo........oooOOOOOooo......

void B1ActionInitialization::BuildForMaster() const
{
  B1RunAction* runAction = new B1RunAction;
  SetUserAction(runAction);
```

```
}
//....oooOOOOOooo........oooOOOOOooo........oooOOOOOooo........oooOOOOOooo......

void B1ActionInitialization::Build() const
{
  SetUserAction(new B1PrimaryGeneratorAction);

  B1RunAction* runAction = new B1RunAction;
  SetUserAction(runAction);

  B1EventAction* eventAction = new B1EventAction(runAction);
  SetUserAction(eventAction);
  SetUserAction(new B1SteppingAction(eventAction));
}
//....oooOOOOOooo........oooOOOOOooo........oooOOOOOooo........oooOOOOOooo......
```

Appendix 2: B1DetectorConstruction.cc – CZT/ CZT in water

```
//
// ********************************************************************
// * License and Disclaimer                                           *
// *                                                                  *
// * The  Geant4 software  is  copyright of the Copyright Holders  of *
// * the Geant4 Collaboration.  It is provided  under  the terms  and *
// * conditions of the Geant4 Software License,  included in the file *
// * LICENSE and available at  http://cern.ch/geant4/license .  These *
// * include a list of copyright holders.                             *
// *                                                                  *
// * Neither the authors of this software system, nor their employing *
// * institutes,nor the agencies providing financial support for this *
// * work  make  any representation or  warranty, express or implied, *
// * regarding  this  software system or assume any liability for its *
// * use.  Please see the license in the file  LICENSE  and URL above *
// * for the full disclaimer and the limitation of liability.         *
// *                                                                  *
// * This  code  implementation is the result of  the  scientific and *
// * technical work of the GEANT4 collaboration.                      *
// * By using,  copying,  modifying or  distributing the software (or *
// * any work based  on the software)  you  agree  to acknowledge its *
// * use  in  resulting  scientific  publications,  and indicate your *
// * acceptance of all terms of the Geant4 Software license.          *
// ********************************************************************
//
//
/// \file B1DetectorConstruction.cc
/// \brief Implementation of the B1DetectorConstruction class

#include "B1DetectorConstruction.hh"

#include "G4RunManager.hh"
#include "G4NistManager.hh"
#include "G4Box.hh"
#include "G4Cons.hh"
#include "G4Orb.hh"
#include "G4Sphere.hh"
#include "G4Trd.hh"
#include "G4LogicalVolume.hh"
#include "G4PVPlacement.hh"
#include "G4SystemOfUnits.hh"

//....oooOOOOOooo........oooOOOOOooo........oooOOOOOooo........oooOOOOOooo......

B1DetectorConstruction::B1DetectorConstruction()
: G4VUserDetectorConstruction(),
  fScoringVolume(0)
{ }

//....oooOOOOOooo........oooOOOOOooo........oooOOOOOooo........oooOOOOOooo......

B1DetectorConstruction::~B1DetectorConstruction()
```

```
{ }

//....oooOOOOOooo........oooOOOOOooo........oooOOOOOooo........oooOOOOOooo......

G4VPhysicalVolume* B1DetectorConstruction::Construct()
{
  // Get nist material manager
  G4NistManager* nist = G4NistManager::Instance();

  // Envelope parameters
  //
  G4double env_sizeXY = 10*mm, env_sizeZ = 10*mm;
  //G4Material* env_mat = nist->FindOrBuildMaterial("G4_AIR");

  //
  //CZT Detector Material
  //

  G4double z, a, density;
  G4String symbol;
  G4int ncomponents, natoms;

  a = 112.41*g/mole;
  G4Element* elCd = new G4Element ("Cadmium", symbol="Cd", z=48., a);

  a = 65.38*g/mole;
  G4Element* elZn = new G4Element ("Zinc", symbol="Zn", z=30., a);

  a=127.60*g/mole;
  G4Element* elTe = new G4Element ("Tellurium", symbol="Te", z=52., a);

  density = 5.76*g/cm3;
  G4Material* CZT_mat = new G4Material ("CdZnTe", density, ncomponents = 3);
  CZT_mat->AddElement(elCd, natoms = 1);
  CZT_mat->AddElement(elZn, natoms = 1);
  CZT_mat->AddElement(elTe, natoms = 1);

  // Option to switch on/off checking of volumes overlaps
  //
  G4bool checkOverlaps = true;

  //
  // World
  //
  G4double world_sizeXY = 1.2*env_sizeXY;
  G4double world_sizeZ  = 1.2*env_sizeZ;
  G4Material* world_mat = nist->FindOrBuildMaterial("G4_AIR"); //use “G4_WATER” for case 2

  G4Box* solidWorld =
    new G4Box("World",                       //its name
       1.0*world_sizeXY, 1.0*world_sizeXY, 1.0*world_sizeZ);     //its size

  G4LogicalVolume* logicWorld =
    new G4LogicalVolume(solidWorld,          //its solid
                        world_mat,           //its material
                        "World");            //its name

  G4VPhysicalVolume* physWorld =
    new G4PVPlacement(0,                     //no rotation
                      G4ThreeVector(),       //at (0,0,0)
                      logicWorld,            //its logical volume
                      "World",               //its name
                      0,                     //its mother  volume
                      false,                 //no boolean operation
                      0,                     //copy number
                      checkOverlaps);        //overlaps checking

  //
  // Envelope
```

```
  //
  G4Box* solidEnv =
    new G4Box("Envelope",                    //its name
        0.5*env_sizeXY, 0.5*env_sizeXY, 0.5*env_sizeZ); //its size

  G4LogicalVolume* logicEnv =
    new G4LogicalVolume(solidEnv,            //its solid
                        CZT_mat,             //its material
                        "Envelope");         //its name

  new G4PVPlacement(0,                       //no rotation
                    G4ThreeVector(),         //at (0,0,0)
                    logicEnv,                //its logical volume
                    "Envelope",              //its name
                    logicWorld,              //its mother  volume
                    false,                   //no boolean operation
                    0,                       //copy number
                    checkOverlaps);          //overlaps checking

  // Set Envelope as scoring volume
  //
  fScoringVolume = logicEnv;

  //
  //always return the physical World
  //
  return physWorld;
}
//....oooOOOOOooo........oooOOOOOooo........oooOOOOOooo........oooOOOOOooo......
```

Appendix 3: B1DetectorConstruction.cc - HPGe

```
//
// ********************************************************************
// * License and Disclaimer                                           *
// *                                                                  *
// * The  Geant4 software  is  copyright of the Copyright Holders  of *
// * the Geant4 Collaboration.  It is provided  under  the terms  and *
// * conditions of the Geant4 Software License,  included in the file *
// * LICENSE and available at  http://cern.ch/geant4/license .  These *
// * include a list of copyright holders.                             *
// *                                                                  *
// * Neither the authors of this software system, nor their employing *
// * institutes,nor the agencies providing financial support for this *
// * work  make  any representation or  warranty, express or implied, *
// * regarding  this  software system or assume any liability for its *
// * use.  Please see the license in the file  LICENSE  and URL above *
// * for the full disclaimer and the limitation of liability.         *
// *                                                                  *
// * This  code  implementation is the result of  the  scientific and *
// * technical work of the GEANT4 collaboration.                      *
// * By using,  copying,  modifying or  distributing the software (or *
// * any work based  on the software)  you  agree  to acknowledge its *
// * use  in  resulting  scientific  publications,  and indicate your *
// * acceptance of all terms of the Geant4 Software license.          *
// ********************************************************************
//
//
/// \file B1DetectorConstruction.cc
/// \brief Implementation of the B1DetectorConstruction class

#include "B1DetectorConstruction.hh"

#include "G4RunManager.hh"
#include "G4NistManager.hh"
#include "G4Box.hh"
#include "G4Cons.hh"
#include "G4Orb.hh"
#include "G4Sphere.hh"
#include "G4Trd.hh"
#include "G4LogicalVolume.hh"
#include "G4PVPlacement.hh"
#include "G4SystemOfUnits.hh"
#include "G4Tubs.hh"

//....oooOOOOOooo........oooOOOOOooo........oooOOOOOooo........oooOOOOOooo......

B1DetectorConstruction::B1DetectorConstruction()
: G4VUserDetectorConstruction(),
  fScoringVolume(0)
{ }

//....oooOOOOOooo........oooOOOOOooo........oooOOOOOooo........oooOOOOOooo......

B1DetectorConstruction::~B1DetectorConstruction()
{ }

//....oooOOOOOooo........oooOOOOOooo........oooOOOOOooo........oooOOOOOooo......

G4VPhysicalVolume* B1DetectorConstruction::Construct()
{
  // Get nist material manager
  G4NistManager* nist = G4NistManager::Instance();

  // Envelope parameters
  //
  G4double env_sizeXY = 10*cm, env_sizeZ = 10*cm;
  G4Material* env_mat = nist->FindOrBuildMaterial("G4_Ge");
```

```
  G4double pi = 3.14159265358979323846;
  G4double pRMin = 0.2*cm, pRMax = 2.5*cm, pDz = 2.1*cm, pSPhi = 0., pDPhi = 2*pi;

  // Option to switch on/off checking of volumes overlaps
  //
  G4bool checkOverlaps = true;

  //
  // World
  //
  G4double world_sizeXY = 1.2*env_sizeXY;
  G4double world_sizeZ  = 1.2*env_sizeZ;
  G4Material* world_mat = nist->FindOrBuildMaterial("G4_AIR");

  G4Box* solidWorld =
    new G4Box("World",                       //its name
       0.5*world_sizeXY, 0.5*world_sizeXY, 0.5*world_sizeZ);     //its size

  G4LogicalVolume* logicWorld =
    new G4LogicalVolume(solidWorld,          //its solid
                        world_mat,           //its material
                        "World");            //its name

  G4VPhysicalVolume* physWorld =
    new G4PVPlacement(0,                     //no rotation
                      G4ThreeVector(),       //at (0,0,0)
                      logicWorld,            //its logical volume
                      "World",               //its name
                      0,                     //its mother  volume
                      false,                 //no boolean operation
                      0,                     //copy number
                      checkOverlaps);        //overlaps checking

  //
  // Envelope
  //
/----------------Define Cylinderical Detector-----------------/

  G4Tubs* solidEnv =
    new G4Tubs("Envelope",                    //its name
        pRMin, pRMax, pDz, pSPhi, pDPhi);    //its size*/


    G4LogicalVolume* logicEnv =
    new G4LogicalVolume(solidEnv,            //its solid
                        env_mat,             //its material
                        "Envelope");         //its name

  new G4PVPlacement(0,                       //no rotation
                    G4ThreeVector(),         //at (0,0,0)
                    logicEnv,                //its logical volume
                    "Envelope",              //its name
                    logicWorld,              //its mother  volume
                    false,                   //no boolean operation
                    0,                       //copy number
                    checkOverlaps);          //overlaps checking

  // Set Envelope as scoring volume
  //
  fScoringVolume = logicEnv;

  //
  //always return the physical World
  //
  return physWorld;
}
//....oooOOOOOooo.........oooOOOOOooo.........oooOOOOOooo.........oooOOOOOooo.....
```

Appendix 4: B1EventAction.cc

```
//
// ********************************************************************
// * License and Disclaimer                                           *
// *                                                                  *
// * The  Geant4 software  is  copyright of the Copyright Holders  of *
// * the Geant4 Collaboration.  It is provided  under  the terms  and *
// * conditions of the Geant4 Software License,  included in the file *
// * LICENSE and available at  http://cern.ch/geant4/license .  These *
// * include a list of copyright holders.                             *
// *                                                                  *
// * Neither the authors of this software system, nor their employing *
// * institutes,nor the agencies providing financial support for this *
// * work  make  any representation or  warranty, express or implied, *
// * regarding  this  software system or assume any liability for its *
// * use.  Please see the license in the file  LICENSE  and URL above *
// * for the full disclaimer and the limitation of liability.         *
// *                                                                  *
// * This  code  implementation is the result of  the  scientific and *
// * technical work of the GEANT4 collaboration.                      *
// * By using,  copying,  modifying or  distributing the software (or *
// * any work based  on the software)  you  agree  to acknowledge its *
// * use  in  resulting  scientific  publications,  and indicate your *
// * acceptance of all terms of the Geant4 Software license.          *
// ********************************************************************
//
//
/// \file B1EventAction.cc
/// \brief Implementation of the B1EventAction class

#include "B1EventAction.hh"
#include "B1RunAction.hh"
#include "B1Analysis.hh"

#include "G4Event.hh"
#include "G4RunManager.hh"

//....oooOOOOOooo........oooOOOOOooo........oooOOOOOooo........oooOOOOOooo......

B1EventAction::B1EventAction(B1RunAction* runAction)
: G4UserEventAction(),
  fRunAction(runAction),
  fEdep(0.)
{}

//....oooOOOOOooo........oooOOOOOooo........oooOOOOOooo........oooOOOOOooo......

B1EventAction::~B1EventAction()
{}

//....oooOOOOOooo........oooOOOOOooo........oooOOOOOooo........oooOOOOOooo......

void B1EventAction::BeginOfEventAction(const G4Event*)
{
  fEdep = 0.;
}

//....oooOOOOOooo........oooOOOOOooo........oooOOOOOooo........oooOOOOOooo......

void B1EventAction::EndOfEventAction(const G4Event*)
{
  // accumulate statistics in run action
  fRunAction->AddEdep(fEdep);

  // Get analysis manager
  G4AnalysisManager* analysisManager = G4AnalysisManager::Instance();

  // Fill ntuple
```

```
  analysisManager->FillNtupleDColumn(0, fEdep);
  analysisManager->AddNtupleRow();

  // Fill histograms
  analysisManager->FillH1(0, fEdep);
}

//....oooOOOOOooo........oooOOOOOooo........oooOOOOOooo........oooOOOOOooo......
```

Appendix 5:B1PrimaryGeneratorAction.cc – CZT/ CZT in water

```
//
// ********************************************************************
// * License and Disclaimer                                           *
// *                                                                  *
// * The  Geant4 software  is  copyright of the Copyright Holders  of *
// * the Geant4 Collaboration.  It is provided  under  the terms  and *
// * conditions of the Geant4 Software License,  included in the file *
// * LICENSE and available at  http://cern.ch/geant4/license .  These *
// * include a list of copyright holders.                             *
// *                                                                  *
// * Neither the authors of this software system, nor their employing *
// * institutes,nor the agencies providing financial support for this *
// * work  make  any representation or  warranty, express or implied, *
// * regarding  this  software system or assume any liability for its *
// * use.  Please see the license in the file  LICENSE  and URL above *
// * for the full disclaimer and the limitation of liability.         *
// *                                                                  *
// * This  code  implementation is the result of  the  scientific and *
// * technical work of the GEANT4 collaboration.                      *
// * By using,  copying,  modifying or  distributing the software (or *
// * any work based  on the software)  you  agree  to acknowledge its *
// * use  in  resulting  scientific  publications,  and indicate your *
// * acceptance of all terms of the Geant4 Software license.          *
// ********************************************************************
//
//
/// \file B1PrimaryGeneratorAction.cc
/// \brief Implementation of the B1PrimaryGeneratorAction class

#include "B1PrimaryGeneratorAction.hh"

#include "G4LogicalVolumeStore.hh"
#include "G4LogicalVolume.hh"
#include "G4Box.hh"
#include "G4Tubs.hh"
#include "G4Event.hh"
#include "G4RunManager.hh"
#include "G4ParticleGun.hh"
#include "G4GeneralParticleSource.hh"
#include "G4ParticleTable.hh"
#include "G4ParticleDefinition.hh"
#include "G4SystemOfUnits.hh"
#include "Randomize.hh"

//....oooOOOOOooo........oooOOOOOooo........oooOOOOOooo........oooOOOOOooo......

B1PrimaryGeneratorAction::B1PrimaryGeneratorAction()
: G4VUserPrimaryGeneratorAction(),
  fParticleGun(0),
  fEnvelopeBox(0)
{
  G4int n_particle = 1;
  fParticleGun  = new G4ParticleGun(n_particle);

  // default particle kinematic
  G4ParticleTable* particleTable = G4ParticleTable::GetParticleTable();
  G4String particleName;
  G4ParticleDefinition* particle
    = particleTable->FindParticle(particleName="gamma");
  fParticleGun->SetParticleDefinition(particle);
  fParticleGun->SetParticleMomentumDirection(G4ThreeVector(0.,0.,1.*cm));
  fParticleGun->SetParticleEnergy(6.*MeV);

}

//....oooOOOOOooo........oooOOOOOooo........oooOOOOOooo........oooOOOOOooo......
```

```
B1PrimaryGeneratorAction::~B1PrimaryGeneratorAction()
{
  delete fParticleGun;
}

//....oooOOOOOooo........oooOOOOOooo........oooOOOOOooo........oooOOOOOooo......

void B1PrimaryGeneratorAction::GeneratePrimaries(G4Event* anEvent)
{
  //this function is called at the begining of each event
  //

  // In order to avoid dependence of PrimaryGeneratorAction
  // on DetectorConstruction class we get Envelope volume
  // from G4LogicalVolumeStore.

  G4double envSizeXY = 0;
  G4double envSizeZ = 0;

  if (!fEnvelopeBox)
  {
    G4LogicalVolume* envLV
      = G4LogicalVolumeStore::GetInstance()->GetVolume("Envelope");
    //if ( envLV ) fEnvelopeBox = dynamic_cast<G4Box*>(envLV->GetSolid());
    if ( envLV ) fEnvelopeBox = dynamic_cast<G4Box*>(envLV->GetSolid());
  }

  if ( fEnvelopeBox ) {
    envSizeXY = fEnvelopeBox->GetXHalfLength()*2;
    envSizeZ = fEnvelopeBox->GetZHalfLength()*2;
  }
  else  {
    G4ExceptionDescription msg;
    msg << "Envelope volume of box shape not found.\n";
    msg << "Perhaps you have changed geometry.\n";
    msg << "The gun will be place at the center.";
    G4Exception("B1PrimaryGeneratorAction::GeneratePrimaries()",
     "MyCode0002",JustWarning,msg);

  }

  //G4double size = 1.0;
  G4double x0 = envSizeXY * (G4UniformRand()-0.5);
  G4double y0 = envSizeXY * (G4UniformRand()-0.5);
  G4double z0 = -5.5*mm;
  //G4double z0 = fParticleGun->GetParticlePosition().z();

  fParticleGun->SetParticlePosition(G4ThreeVector(x0,y0,z0));

  G4cout << "x0, y0, z0 = " << x0 << ",\t" << y0 << ",\t" << z0 << G4endl;

  fParticleGun->GeneratePrimaryVertex(anEvent);
}



//....oooOOOOOooo........oooOOOOOooo........oooOOOOOooo........oooOOOOOooo......
```

Appendix 6: B1PrimaryGeneratorAction.cc – HPGe

```
//
// ********************************************************************
// * License and Disclaimer                                           *
// *                                                                  *
// * The  Geant4 software  is  copyright of the Copyright Holders  of *
// * the Geant4 Collaboration.  It is provided  under  the terms  and *
// * conditions of the Geant4 Software License,  included in the file *
// * LICENSE and available at  http://cern.ch/geant4/license .  These *
// * include a list of copyright holders.                             *
// *                                                                  *
// * Neither the authors of this software system, nor their employing *
// * institutes,nor the agencies providing financial support for this *
// * work  make  any representation or  warranty, express or implied, *
// * regarding  this  software system or assume any liability for its *
// * use.  Please see the license in the file  LICENSE  and URL above *
// * for the full disclaimer and the limitation of liability.         *
// *                                                                  *
// * This  code  implementation is the result of  the  scientific and *
// * technical work of the GEANT4 collaboration.                      *
// * By using,  copying,  modifying or  distributing the software (or *
// * any work based  on the software)  you  agree  to acknowledge its *
// * use  in  resulting  scientific  publications,  and indicate your *
// * acceptance of all terms of the Geant4 Software license.          *
// ********************************************************************
//
//
/// \file B1PrimaryGeneratorAction.cc
/// \brief Implementation of the B1PrimaryGeneratorAction class

#include "B1PrimaryGeneratorAction.hh"

#include "G4LogicalVolumeStore.hh"
#include "G4LogicalVolume.hh"
#include "G4Box.hh"
#include "G4Tubs.hh"
#include "G4Event.hh"
#include "G4RunManager.hh"
#include "G4ParticleGun.hh"
#include "G4GeneralParticleSource.hh"
#include "G4ParticleTable.hh"
#include "G4ParticleDefinition.hh"
#include "G4SystemOfUnits.hh"
#include "Randomize.hh"

//....oooOOOOOooo........oooOOOOOooo........oooOOOOOooo........oooOOOOOooo......

B1PrimaryGeneratorAction::B1PrimaryGeneratorAction()
  : G4VUserPrimaryGeneratorAction(),
    fParticleSource(nullptr)
{
  fParticleSource  = new G4GeneralParticleSource();
}
//....oooOOOOOooo........oooOOOOOooo........oooOOOOOooo........oooOOOOOooo......

B1PrimaryGeneratorAction::~B1PrimaryGeneratorAction() {
    delete fParticleSource;}
//....oooOOOOOooo........oooOOOOOooo........oooOOOOOooo........oooOOOOOooo......

void B1PrimaryGeneratorAction::GeneratePrimaries(G4Event* anEvent) {
    fParticleSource->GeneratePrimaryVertex(anEvent);
    G4double x0 = anEvent->GetPrimaryVertex(0)->GetX0();
    G4double y0 = anEvent->GetPrimaryVertex(0)->GetY0();
    G4double z0 = anEvent->GetPrimaryVertex(0)->GetZ0();

    G4cout << "x0, y0, z0 = " << x0 << ",\t" << y0 << ",\t" << z0 << G4endl;
}
//....oooOOOOOooo........oooOOOOOooo........oooOOOOOooo........oooOOOOOooo......
```

Appendix 7: B1RunAction.cc

```
//
// ********************************************************************
// * License and Disclaimer                                           *
// *                                                                  *
// * The  Geant4 software  is  copyright of the Copyright Holders  of *
// * the Geant4 Collaboration.  It is provided  under  the terms  and *
// * conditions of the Geant4 Software License,  included in the file *
// * LICENSE and available at  http://cern.ch/geant4/license .  These *
// * include a list of copyright holders.                             *
// *                                                                  *
// * Neither the authors of this software system, nor their employing *
// * institutes,nor the agencies providing financial support for this *
// * work  make  any representation or  warranty, express or implied, *
// * regarding  this  software system or assume any liability for its *
// * use.  Please see the license in the file  LICENSE  and URL above *
// * for the full disclaimer and the limitation of liability.         *
// *                                                                  *
// * This  code  implementation is the result of  the  scientific and *
// * technical work of the GEANT4 collaboration.                      *
// * By using,  copying,  modifying or  distributing the software (or *
// * any work based  on the software)  you  agree  to acknowledge its *
// * use  in  resulting  scientific  publications,  and indicate your *
// * acceptance of all terms of the Geant4 Software license.          *
// ********************************************************************
//
//
/// \file B1RunAction.cc
/// \brief Implementation of the B1RunAction class

#include "B1RunAction.hh"
#include "B1PrimaryGeneratorAction.hh"
#include "B1DetectorConstruction.hh"
#include "B1Analysis.hh"
// #include "B1Run.hh"

#include "G4RunManager.hh"
#include "G4Run.hh"
#include "G4AccumulableManager.hh"
#include "G4LogicalVolumeStore.hh"
#include "G4LogicalVolume.hh"
#include "G4UnitsTable.hh"
#include "G4SystemOfUnits.hh"

//....oooOOOOOooo........oooOOOOOooo........oooOOOOOooo........oooOOOOOooo......

B1RunAction::B1RunAction()
: G4UserRunAction(),
  fEdep(0.),
  fEdep2(0.)
{
  // add new units for dose
  //
  const G4double milligray = 1.e-3*gray;
  const G4double microgray = 1.e-6*gray;
  const G4double nanogray  = 1.e-9*gray;
  const G4double picogray  = 1.e-12*gray;

  new G4UnitDefinition("milligray", "milliGy" , "Dose", milligray);
  new G4UnitDefinition("microgray", "microGy" , "Dose", microgray);
  new G4UnitDefinition("nanogray" , "nanoGy"  , "Dose", nanogray);
  new G4UnitDefinition("picogray" , "picoGy"  , "Dose", picogray);

  // Register accumulable to the accumulable manager
  G4AccumulableManager* accumulableManager = G4AccumulableManager::Instance();
  accumulableManager->RegisterAccumulable(fEdep);
  accumulableManager->RegisterAccumulable(fEdep2);
}
```

```
//....oooOOOOOooo........oooOOOOOooo........oooOOOOOooo........oooOOOOOooo......

B1RunAction::~B1RunAction()
{}

//....oooOOOOOooo........oooOOOOOooo........oooOOOOOooo........oooOOOOOooo......

void B1RunAction::BeginOfRunAction(const G4Run* aRun)
{
  // inform the runManager to save random number seed
  G4RunManager::GetRunManager()->SetRandomNumberStore(false);

  // reset accumulables to their initial values
  G4AccumulableManager* accumulableManager = G4AccumulableManager::Instance();
  accumulableManager->Reset();

  // Create/get analysis manager

  G4AnalysisManager* analysisManager = G4AnalysisManager::Instance();
  analysisManager->SetVerboseLevel(1);

  char EdepNtuple[65];
  sprintf(EdepNtuple, "EdepNTuples_run%04d", aRun->GetRunID());
  analysisManager->SetFileName(G4String(EdepNtuple));
  analysisManager->OpenFile();

  // Open an output file
  //analysisManager->OpenFile("EdepTuples");

  // Creation of ntuple
  analysisManager->CreateNtuple("EdepNtuple", "Edep");

  // X = D in CreateNtupleXColumn stands for G4double (I,F,D,S)
  analysisManager->CreateNtupleDColumn("Edep");
  analysisManager->FinishNtuple();

  // Create histograms
  analysisManager->CreateH1("Edep","Energy deposit", 50, 0., 12.*MeV);

}

//....oooOOOOOooo........oooOOOOOooo........oooOOOOOooo........oooOOOOOooo......

void B1RunAction::EndOfRunAction(const G4Run* run)
{
  // Get analysis manager
  G4AnalysisManager* analysisManager = G4AnalysisManager::Instance();

  // Write and close the output file
  analysisManager->Write();
  analysisManager->CloseFile();

  G4int nofEvents = run->GetNumberOfEvent();
  if (nofEvents == 0) return;

  // Merge accumulables
  G4AccumulableManager* accumulableManager = G4AccumulableManager::Instance();
  accumulableManager->Merge();

  // Compute dose = total energy deposit in a run and its variance
  //
  G4double edep  = fEdep.GetValue();
  G4double edep2 = fEdep2.GetValue();

  G4double rms = edep2 - edep*edep/nofEvents;
  if (rms > 0.) rms = std::sqrt(rms); else rms = 0.;

  const B1DetectorConstruction* detectorConstruction
```

```
   = static_cast<const B1DetectorConstruction*>
     (G4RunManager::GetRunManager()->GetUserDetectorConstruction());
  G4double mass = detectorConstruction->GetScoringVolume()->GetMass();
  G4double dose = edep/mass;
  G4double rmsDose = rms/mass;

  // Run conditions
  //  note: There is no primary generator action object for "master"
  //        run manager for multi-threaded mode.
  const B1PrimaryGeneratorAction* generatorAction
   = static_cast<const B1PrimaryGeneratorAction*>
     (G4RunManager::GetRunManager()->GetUserPrimaryGeneratorAction());
  G4String runCondition;
  if (generatorAction)
  {
    const G4ParticleGun* particleGun = generatorAction->GetParticleGun();
    //const G4GeneralParticleSource* particleGun = generatorAction->GetParticleGun();
    runCondition += particleGun->GetParticleDefinition()->GetParticleName();
    runCondition += " of ";
    G4double particleEnergy = particleGun->GetParticleEnergy();
    runCondition += G4BestUnit(particleEnergy,"Energy");
  }

  // Print
  //
  if (IsMaster()) {
    G4cout
     << G4endl
     << "--------------------End of Global Run-----------------------";
  }
  else {
    G4cout
     << G4endl
     << "--------------------End of Local Run-----------------------";
  }

  G4cout
     << G4endl
     << " The run consists of " << nofEvents << " "<< runCondition
     << G4endl
     << " Cumulated dose per run, in scoring volume : "
     << G4BestUnit(dose,"Dose") << " rms = " << G4BestUnit(rmsDose,"Dose")
     << G4endl
     << "------------------------------------------------------------"
     << G4endl
     << G4endl;
}

//....oooOOOOOooo........oooOOOOOooo........oooOOOOOooo........oooOOOOOooo......

void B1RunAction::AddEdep(G4double edep)
{
  fEdep  += edep;
  fEdep2 += edep*edep;
}


//....oooOOOOOooo........oooOOOOOooo........oooOOOOOooo........oooOOOOOooo......
```

Appendix 8: B1SteppingAction

```
//
// ********************************************************************
// * License and Disclaimer                                           *
// *                                                                  *
// * The  Geant4 software  is  copyright of the Copyright Holders  of *
// * the Geant4 Collaboration.  It is provided  under  the terms  and *
// * conditions of the Geant4 Software License,  included in the file *
// * LICENSE and available at  http://cern.ch/geant4/license .  These *
// * include a list of copyright holders.                             *
// *                                                                  *
// * Neither the authors of this software system, nor their employing *
// * institutes,nor the agencies providing financial support for this *
// * work  make  any representation or  warranty, express or implied, *
// * regarding  this  software system or assume any liability for its *
// * use.  Please see the license in the file  LICENSE  and URL above *
// * for the full disclaimer and the limitation of liability.         *
// *                                                                  *
// * This  code  implementation is the result of  the  scientific and *
// * technical work of the GEANT4 collaboration.                      *
// * By using,  copying,  modifying or  distributing the software (or *
// * any work based  on the software)  you  agree  to acknowledge its *
// * use  in  resulting  scientific  publications,  and indicate your *
// * acceptance of all terms of the Geant4 Software license.          *
// ********************************************************************
//
//
/// \file B1SteppingAction.cc
/// \brief Implementation of the B1SteppingAction class

#include "B1SteppingAction.hh"
#include "B1EventAction.hh"
#include "B1DetectorConstruction.hh"

#include "G4Step.hh"
#include "G4Event.hh"
#include "G4RunManager.hh"
#include "G4LogicalVolume.hh"

//....oooOOOOOooo........oooOOOOOooo........oooOOOOOooo........oooOOOOOooo......

B1SteppingAction::B1SteppingAction(B1EventAction* eventAction)
: G4UserSteppingAction(),
  fEventAction(eventAction),
  fScoringVolume(0)
{}

//....oooOOOOOooo........oooOOOOOooo........oooOOOOOooo........oooOOOOOooo......

B1SteppingAction::~B1SteppingAction()
{}

//....oooOOOOOooo........oooOOOOOooo........oooOOOOOooo........oooOOOOOooo......

void B1SteppingAction::UserSteppingAction(const G4Step* step)
{
  if (!fScoringVolume) {
    const B1DetectorConstruction* detectorConstruction
      = static_cast<const B1DetectorConstruction*>
        (G4RunManager::GetRunManager()->GetUserDetectorConstruction());
    fScoringVolume = detectorConstruction->GetScoringVolume();
  }

  // get volume of the current step
  G4LogicalVolume* volume
    = step->GetPreStepPoint()->GetTouchableHandle()
      ->GetVolume()->GetLogicalVolume();
```

```
  // check if we are in scoring volume
  if (volume != fScoringVolume) return;

  // collect energy deposited in this step
  G4double edepStep = step->GetTotalEnergyDeposit();
  fEventAction->AddEdep(edepStep);
}

//....oooOOOOOooo........oooOOOOOooo........oooOOOOOooo........oooOOOOOooo......
```

Appendix 9: HPGeAutoRun.mac

```
# automate run using GeneralParticleSource (GPS)
/gps/particle gamma
/gps/pos/type Volume
/gps/pos/shape Cylinder
/gps/pos/centre 0. 0. 0. cm
/gps/pos/confine Envelope
/gps/pos/radius 2.5 cm
/gps/pos/inner_radius 0.2 cm
/gps/pos/halfz 2.1 cm
#/gps/ang/type iso
/gps/energy {eKin} keV
/gps/number 1
/vis/scene/endOfEventAction accumulate
/run/beamOn 100000
```

Appendix 10: KromekAutoRun.mac

```
# automate run for specified (eKin) gamma energies
#
/gun/particle gamma
/gun/energy {eKin} keV
/run/beamOn 100000
```

Appendix 11: run1.mac

```
# Macro file for example B1
#
# Can be run in batch, without graphic
# or interactively: Idle> /control/execute run1.mac
#
# Change the default number of workers (in multi-threading mode)
#/run/numberOfThreads 4
#
# Initialize kernel
/run/initialize
#
/control/verbose 0
/control/macroPath <dir containing autorun file>/AutoRunFile.mac
/run/verbose 0
/event/verbose 0
/tracking/verbose 1

/control/foreach AutoRunFile.mac eKin "25, 50, 75, 100, 125, 150, 175, 200, 225, 250, 275, 300, 325,
350, 375, 400, 440, 480, 520, 560, 600, 650, 700, 750, 800, 850, 900, 1000, 1100, 1200, 1300, 1400,
1600, 1800, 2100, 2400, 2700, 3000"

#uncomment line for ~662 keV simulation
#/control/foreach AutoRunFile.mac eKin "661.659”

/run/printProgress 100
```

Appendix 12: draw662keV.C

```
{
  TCanvas *c1 = new TCanvas();

  TFile *f1 = new TFile("EdepNtuples_Kromek_662keV.root","READ");
  TTree *t1 = (TTree*)f1->Get("EdepNtuple");
  t1->SetName("EdepNtuple_Kromek");
  TH1 *hist1 = new TH1F("hist1","E_{dep} distribution, CZT ~662 keV;E_{dep};counts",110,0,0.7315);
  hist1->SetLineWidth(2);
  t1->Draw("Edep>>hist1");
  c1->SetLogy(1);
  c1->Print("Edep_662keV_Kromek.png");
  float eff1 = hist1->Integral(99,101)*1.0/hist1->Integral(1,110);
  float err1 = eff1*sqrt(1.0/hist1->Integral(99,101) + 1.0/hist1->Integral(1,110));
  cerr << "Kromek efficiency: " << eff1 << " +- " << err1 << endl;


  TFile *f2 = new TFile("EdepNtuples_HPGe_662keV.root","READ");
  TTree *t2 = (TTree*)f2->Get("EdepNtuple");
  t2->SetName("EdepNtuple_HPGe");
  TH1 *hist2 = new TH1F("hist2","E_{dep} distribution, HPGe ~662 keV;E_{dep};counts",110,0,0.7315);
  hist2->SetLineWidth(2);
  t2->Draw("Edep>>hist2");
  c1->Print("Edep_662keV_HPGe.png");
  float eff2 = hist2->Integral(99,101)*1.0/hist1->Integral(1,110);
  float err2 = eff2*sqrt(1.0/hist2->Integral(99,101) + 1.0/hist2->Integral(1,110));
  cerr << "HPGe efficiency: " << eff2 << " +- " << err2 << endl;
}
```

Appendix 13: DrawAllE.C

```
//
const char * filename = "EdepNtuples_all_Kromek.root";
const char * figstring = "Kromek";
const int NE = 38;
float E[NE] = {50, 25, 50, 75, 100, 125, 150, 175, 200, 225, 250, 275, 300, 325, 350, 375, 400, 440,
480, 520, 560, 600, 650, 700, 750, 800, 850, 900, 1000, 1100, 1200, 1300, 1400, 1600, 1800, 2100,
2400, 2700};
int doPlot[NE] = {1, 1, 1, 1, 1, 1, 1, 1, 1, 1, 1, 1, 1, 1, 1, 1, 1, 1, 1, 1, 1, 1, 1, 1, 1, 1, 1,
1, 1, 1, 1, 1, 1, 1, 1, 1, 1, 1};
TF1 *myfunc = new TF1("myfunc","TMath::Min(1.0,([0]*[2])*TMath::Power(x,-[1])*(1-exp(-
TMath::Power(x,[1])/[2]))*(1+[3]*x))",22,3100);

void DrawAllE()
{
  TCanvas *c = new TCanvas();
  c->SetLogy(1);
  TFile *f = new TFile(filename,"READ");
  TTree *t[NE];
  for(int iE=0; iE<NE; iE++)
  {
    t[iE] = (TTree*)f->Get(Form("EdepNtuple_E%02d",iE));
  }
  TH1 *hist[NE];
  for(int iE=0; iE<NE; iE++)
  {
    // The histogram should have e.g. 110 bins from 0 to Emax, with Emax = E*1.1/0.995, so that the
full energy peak is centered in the center of the 100th bin (99.5)
    hist[iE] = new TH1F(Form("hist_E%02d",iE),"E_{dep}/E_{in}
distribution;E_{dep}/E_{in};counts",110,0,1.1/0.995);
    hist[iE]->SetLineWidth(2);
    t[iE]->Draw(Form("Edep*1000./%.0f>>hist_E%02d",E[iE],iE));
    hist[iE]->SetMinimum(0.5);
    hist[iE]->SetMaximum(5e5);
  }
  c->Clear();
  gStyle->SetOptStat(0);
  TLegend *leg = new TLegend(0.87,0.01,0.99,0.99);

  float eff[NE] = {0};
  float err[NE] = {0};
  float errX[NE] = {0};
  for(int iE=0; iE<NE; iE++)
  {
    hist[iE]->GetXaxis()->CenterTitle(1);
    hist[iE]->GetXaxis()->SetTitleOffset(1.3);
    hist[iE]->SetLineColor(iE%9+1);
    hist[iE]->SetLineStyle(iE%8+1);
    if(true)// doPlot[iE])
    {
      hist[iE]->Draw("SAME");
      leg->AddEntry(hist[iE],Form("E=%.0f keV",E[iE]),"l");
    }
    eff[iE] = hist[iE]->Integral(99,101)*1.0/hist[iE]->Integral(1,110);
    err[iE] = eff[iE]*sqrt(1.0/hist[iE]->Integral(99,101) + 1.0/hist[iE]->Integral(1,110));
    cout << "E = " << E[iE] << " keV case: " << hist[iE]->Integral(99,101) << "/" << hist[iE]-
>Integral(1,110) << " = "
                                          << eff[iE] << " +- " << err[iE]
                                          << ", before peak: " << hist[iE]->Integral(1,99)
                                          << ", after peak: " << hist[iE]->Integral(102,110) <<
endl;
  }

  leg->Draw();

  c->Print(Form("Edep_E_allE_%s.png",figstring));

  c->Clear();
```

```
  c->SetLogx(1);
  c->SetLogy(1);

  TGraphErrors *g = new TGraphErrors(NE,E,eff,errX,err);

  myfunc->SetLineColor(kRed);

  g->SetMarkerColor(kRed);
  g->SetMarkerSize(0.5);
  g->SetMarkerStyle(20);
  g->SetTitle("efficiency vs E_{in}");
  g->GetXaxis()->SetTitle("E_{in} [keV]");
  g->GetYaxis()->SetTitle("efficiency");
  g->GetYaxis()->SetRangeUser(5e-3,5);
  g->Draw("APL");
  c->Print(Form("efficiency_vs_E_%s.png",figstring));
  g->Fit("myfunc","R");
  myfunc->Draw("SAME");
  c->Print(Form("efficiency_vs_E_fit_%s.png",figstring));
}
```

Appendix 14: DrawEffPlot.C

```
const char * filename[3] = {"eff_vs_E_Kromek.txt", "eff_vs_E_KromekWater.txt", "eff_vs_E_HPGe.txt"};
const char * figstring[3] = {"CZT in air", "CZT in water", "HPGe in air"};
const char * fitfunc[3] = {
"TMath::Min(1.0,([0]*[2])*TMath::Power(x,-[1])*(1-exp(-
TMath::Power(x,[1])/[2]))*(1+[3]*TMath::Power(x,1.00)))",
"TMath::Min(1.0,([0]*[2])*TMath::Power(x,-[1])*(1-exp(-
TMath::Power(x,[1])/[2]))*(1+[3]*TMath::Power(x,1.00)))",
"TMath::Min(1.0,([0]*[2])*TMath::Power(x,-[1])*(1-exp(-
TMath::Power(x,[1])/[2]))*(1+[3]*TMath::Power(x,0.75)))"};
int colors[3] = {2, 1, 4};
int markers[3] = {20, 24, 21};

void DrawEffPlot()
{
  TCanvas *c = new TCanvas("c","c",1024,768);
  c->SetLogx(1);
  c->SetLogy(1);

  TLegend *l = new TLegend(0.55,0.6,0.9,0.9);

  TGraphErrors *g[3];
  TF1 *myfunc[3];
  for(int ig=0; ig<3; ig++)
  {
    g[ig] = new TGraphErrors(filename[ig],"%lg %lg %lg");

    myfunc[ig] = new TF1(Form("myfunc%d",ig),fitfunc[ig],24,3100);
    myfunc[ig]->SetParameters(1,2,1e4,1e-3);
    myfunc[ig]->SetLineColor(colors[ig]);
    g[ig]->Fit(Form("myfunc%d",ig),"R");

    g[ig]->SetMarkerColor(colors[ig]);
    g[ig]->SetMarkerSize(1);
    g[ig]->SetMarkerStyle(markers[ig]);
    g[ig]->SetTitle("efficiency vs E_{in}");
    g[ig]->GetXaxis()->SetTitle("E_{in} [keV]");
    g[ig]->GetYaxis()->SetTitle("efficiency");
    g[ig]->GetYaxis()->SetRangeUser(5e-3,5);
    if(ig==0) g[ig]->Draw("AP");
    else g[ig]->Draw("P");
    myfunc[ig]->Draw("SAME");
    l->AddEntry(g[ig],figstring[ig],"PE");
  }
  l->Draw();
  c->Print("efficiency_vs_E_fit_all.png");
}
```

Appendix 15: DrawGausFit

```
void drawGausFit(){

 TGraphErrors *g = new TGraphErrors("MeasurementOutputFile.txt");

 TCanvas *c = new TCanvas();

 TF1 *f1 = new TF1("f1","gaus",882,900.);

 g->Fit("f1","R");

 g->SetMarkerColor(kBlack);
 g->SetMarkerSize(0.5);
 g->SetMarkerStyle(20);
 g->SetTitle("Spectrum");
 g->GetXaxis()->SetTitle("channel number");
 g->GetYaxis()->SetTitle("counts");

 g->GetXaxis()->SetRangeUser(0,1000);
 g->Draw("ALP");
 c->Print("specrum_data.png");

 g->GetXaxis()->SetRangeUser(800,1000);

 g->Draw("ALP");
 f1->SetLineWidth(2);
 f1->DrawCopy("SAME");
 f1->SetLineWidth(1);
 f1->SetRange(500,1000);
 f1->DrawCopy("SAME");
 c->Print("gaussian_data_fit.png");

}
```